nature communications

Article

https://doi.org/10.1038/s41467-025-61992-8

Enrichment of decidual CD11c + CD8 + T cells with altered immune function in early pregnancy loss

Received: 6 October 2024

Accepted: 7 July 2025

Published online: 21 July 2025

Check for updates

Ling Guo[1,2,3], Anliang Guo[1,3], Yaqiu Guo[4], Shuwen Han[1,3], Cameron Klein[1], Zi-Jiang Chen[1] ✉, Junhao Yan[1] ✉ & Yan Li[1,3] ✉

Early pregnancy loss (EPL) is closely associated with imbalances in the maternal-foetal immune microenvironment. Here we identify CD11c + CD8 + T cells, an unconventional cytotoxic T cell subset, as significantly enriched and activated in EPL cases. These cells contribute to immune dysregulation and inhibit trophoblast invasion through secreting granzyme B, perforin, CD107a, TNF-α, and IFN-γ. Furthermore, we present an effective early prediction model for EPL, based on cytokine and cytotoxic molecule profiles of CD11c + CD8 + T cells in maternal serum, collected 12-16 days post-embryo transfer. Functional assays reveal that IFN-γ triggers trophoblast pyroptosis via the NLRP3/Caspase-1/GSDMD pathway, impairing trophoblast invasion. In vivo validation using abortion-prone mice and an anti-4-1BB antibody-induced model of CD11c + CD8 + T cell activation confirms increased embryo resorption and reduced trophoblast infiltration. These findings highlight the role of dysregulated CD11c + CD8 + T cells at the maternal-foetal interface in EPL, and suggest their potential as biomarkers and therapeutic targets for EPL-management.

Early pregnancy loss (EPL) refers to spontaneous abortion occurring before the 12th week of gestation, accounting for approximately 80% of all cases of pregnancy loss and representing a common adverse pregnancy outcome[1,2]. EPL not only hinders women's fertility desires but also may lead to serious complications such as infection, hemorrhage, and secondary infertility, imposing significant psychological and economic burdens on individuals and families[3]. Therefore, there is urgent need for research on the etiology and mechanisms of EPL to develop targeted and precise diagnostic and therapeutic strategies[4].

At the maternal-fetal interface, many decidual immune cells, including CD8 + T cells, interact with decidual stromal cells or trophoblasts to ensure healthy pregnancy[5,6]. Studies have shown that decidual CD8 + T cells exhibit a non-inflammatory, low cytotoxic state to maintain maternal-fetal immune tolerance during early pregnancy[7]. During a healthy pregnancy, extravillous trophoblast cells (EVT) invade the maternal decidua and express embryo-derived allogeneic human leukocyte antigens, which are recognized by CD8 + T cells. These CD8 + T cells acquire a tolerant phenotype by regulating the degree of inflammation at the maternal-fetal interface, thereby ensuring that the embryo is protected from maternal immune system attack[8]. Additionally, GM-CSF-mediated pregnancy protection relies on CD8 + T cell-dependent suppression of anti-trophoblast natural killer cytotoxicity[9]. Murine studies also demonstrate that stress-induced abortion involves substance P-mediated suppression of immunoprotective CD8 + T cells[10].

Recent studies have confirmed that enrichment of dysfunctional decidual CD8 + T cells is associated with adverse pregnancy outcomes such as EPL and preeclampsia[11,12]. Ghafourian et al. reported a

[1]State Key Laboratory of Reproductive Medicine and Offspring Health, Center for Reproductive Medicine, The Second Hospital, Institute of Women, Children and Reproductive Health, Shandong University, Jinan, Shandong, China. [2]Department of Obstetrics and Gynecology, Qilu Hospital of Shandong University, Jinan, Shandong, China. [3]Medical Integration and Practice Center, Shandong University, Jinan, Shandong, China. [4]Jinan Maternity and Child Care Hospital Affiliated to Shandong First Medical University, Jinan, Shandong, China. ✉e-mail: chenzijiang@hotmail.com; yyy306@126.com; ubcliyan@sdu.edu.cn

significant increase in the proportion of CD8 + T cells in the peripheral blood of women with recurrent pregnancy loss[13]. Similarly, Morita et al. reported an increase in the number of decidual cytotoxic CD8 + T cells in patients with EPL[14]. Studies have also shown that, in abnormal cases, CD8 + T cells can exhibit cytotoxic function by secreting cytolytic molecules such as perforin and granzyme, leading to EPL[15,16]. Most studies on decidual CD8 + T cells are limited to their common immunoregulatory roles; however, in-depth exploration of the abnormal activation and regulatory mechanisms of cytotoxic CD8 + T cells is lacking. As a result, the mechanisms by which these cells contribute to the pathogenesis of EPL have not been fully elucidated.

CD11c, a member of the β integrin family, is a common biomarker of dendritic cells, although it is also expressed in B lymphocyte cells, subsets of CD8 + T cells, and natural killer cells[17]. Several studies have shown that CD11c + CD8 + T cells represent a highly activated, secreted, and cytotoxic effector subset that is widely distributed in the peripheral blood, spleen, liver, and other tissues[18,19]. This subset of cells undergoes expansion in response to antigen stimulation, exhibiting high antigen specificity[20]. In models of autoimmune disease, the activation of CD8 + T cells is accompanied by the upregulation of CD11c[21]. Furthermore, the number of CD11c + CD8 + T cells significantly increases in reproductive tract infections, suggesting their involvement in the body's inflammatory response[20]. Prior to this study, there were no reports on decidual CD11c + CD8 + T cells, making their involvement in EPL unclear.

In this study, we investigate the phenotype and function of CD11c + CD8 + T cells in both decidual tissue and peripheral blood from patients with early pregnancy loss. We show that the enrichment and dysfunction of these cells impair trophoblast behavior and contribute to pregnancy loss. Additionally, we develop a multi-marker predictive model for EPL based on related cytokines and cytotoxic molecules. These findings provide insights into immune regulation at the maternal-fetal interface and offer potential targets for the early prediction and intervention of EPL.

Results

Enrichment of decidual CD11c + CD8 + T cells in patients with EPL

To understand the phenotypic characteristics of decidual immune cells in early pregnancy, we analyzed single-cell RNA sequencing (scRNA-seq) datasets (GSE164449)[22] of CD45+ immune cells from six decidual samples, including three from healthy controls (HC) and three from EPL cases, collected between 6-9 weeks of gestation. The analysis revealed that CD8 + T cells were the predominant T cell subpopulation in the decidua (Fig. 1A–C). Further comparison of differentially expressed genes (DEGs) in CD8 + T cells between the two groups indicated that 142 genes were significantly upregulated in the EPL group compared to the HC group ($P < 0.05$, log2FC > 1), which includes several genes known to be closely associated with the maintenance of normal pregnancy, such as *CCL2*, *CCR2*, *CXCL8*, *IFI27*, and *TIGIT*[23–26] (Fig. 1D). Among these genes, the expression of *ITGAX*, which encodes CD11c, was significantly higher in decidual CD8 + T cells of the EPL group than in those of the HC group (Fig. 1E). Additionally, the data revealed differences in the transcription levels of genes related to T cell cytotoxicity and interferon signaling between EPL and HC derived CD11c + CD8 + T cells, such as *GZMB*, *PRF1*, and *IL2RB* (Fig. 1F). The DEGs in the CD11c + CD8 + T cell subpopulation were primarily enriched in immune regulation-related signaling pathways (Fig. 1G), suggesting that decidual CD11c + CD8 + T cells in EPL patients may exhibit highly activated and immuno-destructive phenotypic characteristics.

To ensure the quality of the scRNA-seq dataset, we performed quality control screening on the dataset, resulting in a total of 13,681 high-quality cells, with 5608 cells from HC decidua and 8073 cells from EPL decidua meeting quality standards (Supplementary Fig. 1A). The principal component analysis (PCA) elbow plot visualization showed similar cell distributions between the two groups, confirming no significant batch differences among the samples (Supplementary Fig. 1B). Using established markers from previous studies[22,27] and machine annotation results, we captured most immune cell types in the decidua, as illustrated in the t-SNE dimensionality reduction plot (Supplementary Fig. 1C). Examination of the expression of marker genes revealed T cells with high expression of CD3D and CD8A in the dataset (Supplementary Fig. 1D–E).

To validate the findings from scRNA-seq analysis, we first investigated the expression pattern of CD11c + CD8 + T cells in the decidua and peripheral blood mononuclear cells (PBMC) of 10 women in HC group. The flow cytometry gating strategy for CD11c + CD8 + T cells in decidua and PBMCs is shown in Fig. 1H. The initial results demonstrated that the proportion of CD11c + CD8 + T cells in the decidua was significantly higher than that in the PBMCs, indicating a specific enrichment of CD11c + CD8 + T cells in the decidua during pregnancy (Fig. 1I). Subsequently, we expanded the decidual sample size to include 18 women in the HC group and 20 women in the EPL group, confirming that the frequency of CD11c + CD8 + T cells in the decidua of the EPL group was significantly higher than that in the HC group (11.22% ± 3.32% vs. 8.05% ± 2.69%, $P = 0.003$) (Fig. 1J). Immunofluorescence staining of human decidual tissue revealed the colocalization of CD11c and CD8, further confirming that CD11c + CD8 + T cells were enriched in the decidua of the EPL group compared to those of the HC group (Fig. 1K). Additionally, an increased frequency of CD11c + CD8 + T cells was also observed in the peripheral blood of EPL patients compared to those in the HC group (7.74% ± 4.10% vs. 4.58% ± 1.96%, $P = 0.041$) (Supplementary Fig. 1F).

CD11c + CD8 + T cells exhibit high activation and strong cytotoxic characteristics in EPL

To further explore the role of CD11c + CD8 + T cells in EPL, we subsequently assessed the distribution of CD11c + CD8 + T cell subtypes based on the co-expression of CD45RA and CCR7. CD45RA is a marker for naive T cells, while CCR7 is associated with T cell migration to secondary lymphoid organs[28]. Interestingly, compared to the HC group, we observed a further increase in the proportion of CCR7-CD45RA+ effector CD8 + T cell subset and a decrease in the CCR7 + CD45RA+ naive CD8 + T cell subset within the decidual CD11c + CD8 + T cells of EPL group (Fig. 2A). Additionally, we measured the expression levels of the activation and immune exhaustion markers HLA-DR, CD38, and PD-1. The results revealed that the expression of HLA-DR and CD38 was significantly higher in CD11c + CD8 + T cells compared to CD11c-CD8 + T cells in both the HC and EPL groups (Fig. 2B). For PD-1 expression, we found that it was significantly lower in both CD11c + CD8 + T cells and CD11c-CD8 + T cells from EPL group compared to the HC group (Fig. 2C). These results indicate that CD11c + CD8 + T cells, as an effector CD8 + T cell subset, are specifically enriched and activated in EPL patients.

The cytotoxic function and cytokine secretion capacity of decidual CD8 + T cells have an important impact on the establishment and maintenance of pregnancy. Based on the above scRNA-seq analysis indicating that CD11c + CD8 + T cells in EPL patients exhibit a transcriptional phenotype associated with cytotoxic functions, we further analyzed the transcriptome sequencing data (GSE183022)[18] of CD11c + CD8 + T cells and CD11c-CD8 + T cells from the peripheral blood of three healthy donors. The analysis revealed that, compared to CD11c-CD8 + T cells, CD11c + CD8 + T cells exhibited significantly higher transcription levels of genes associated with T cell activation and cytotoxic functions (such as *CD38*, *GZMB*, and *PRF1*) (Supplementary Fig. 2A). Gene ontology (GO) and kyoto encyclopedia of genes and genomes (KEGG) enrichment analyses revealed that CD11c + CD8 + T cells were significantly enriched in pathways related to immune activation, the regulation of cell killing, and cytokine secretion (Supplementary Fig. 2B, C). These results suggest that, at the

https://doi.org/10.1038/s41467-025-61992-8

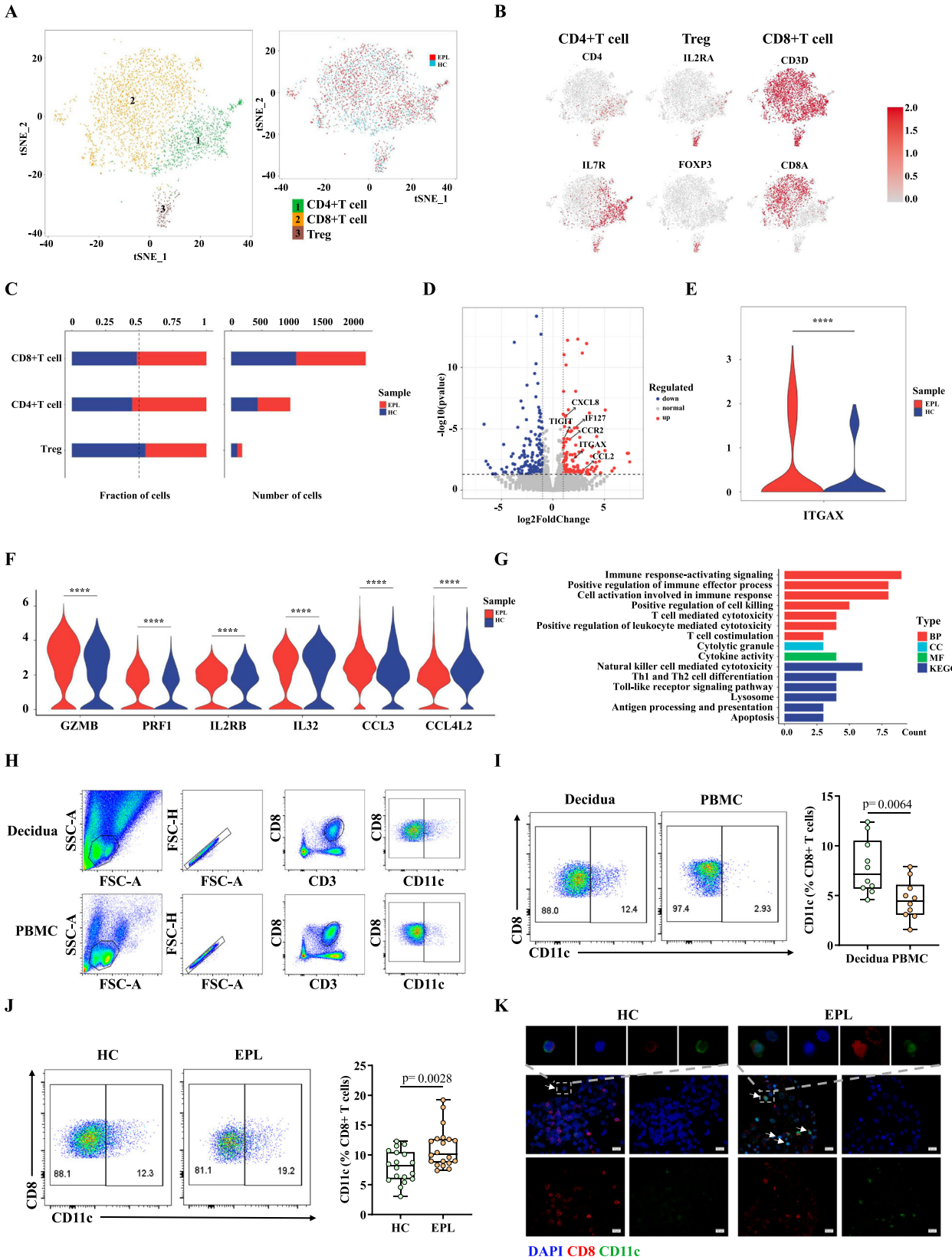

transcriptional level, CD11c + CD8 + T cells represent a highly activated and multifunctional effector CD8 + T cell subpopulation.

Therefore, we further explored the functional characteristics of decidual CD11c + CD8 + T cells in HC and EPL groups. Our results showed that decidual CD11c + CD8 + T cells expressed higher levels of CD107a, granzyme B, perforin, TNF-α, and IFN-γ compared to CD11c- CD8 + T cells (Fig. 2D–G), indicating that CD11c + CD8 + T cells have significant cytokine and cytolytic molecule secretion capacity, which is consistent with the transcriptome sequencing results. We also found that the expression of CD107a, granzyme B, TNF-α, and IFN-γ in decidual CD11c + CD8 + T cells was significantly higher in the EPL group than in the HC group (Fig. 2D–G). In the peripheral blood

Fig. 1 | Enrichment of CD11c + CD8 + T cells in decidua of EPL patients. A t-SNE visualization of dimensionality reduction clustering plot showing three main clusters of decidual CD8 + T cells from 3 EPL patients and 3 HC women. Different colors represent distinct cell clusters and disease states (see legend). **B** t-SNE visualization distribution plot of marker genes used to identify three major decidual CD8 + T cell types. **C** Proportions (left) and numbers (right) of three major subsets of decidual CD8 + T cells from EPL and HC samples. **D** Volcano plot showing differentially expressed genes in decidual CD8 + T cells from EPL and HC. |log2FC| > 1 and *P* value < 0.05 were considered significant. **E** Violin plot depicting higher expression of ITGAX in EPL compared to HC decidual CD8 + T cells. ****$P < 0.0001$. **F** Violin plot displaying differential expression of selected marker genes in CD11c + CD8 + T cells from EPL and HC decidua. ****$P < 0.0001$. **G** GO and KEGG pathway enrichment analysis plot of CD11c + CD8 + T cells from EPL and HC decidua. **H** Typical gating strategy for CD11c + CD8 + T cells in early pregnancy decidua and PBMC. **I** Flow cytometry analysis and quantification of CD11c + CD8 + T cells in PBMC and decidua from healthy early pregnant women ($n = 10$). **J** Flow cytometry detection of CD11c + CD8 + T cell frequency in decidua from HC ($n = 18$) and EPL patients ($n = 20$). Left panel shows typical flow cytometry gating of CD11c on decidual CD8 + T cells. **K** Typical immunofluorescence staining image of CD11c (green), CD8 (red), and DAPI (blue) in decidua from HC and EPL patients. White arrows indicate a single CD11c + CD8 + T cell. Scale bar = 50 μm. Representative results from three independent biological replicates. EPL early pregnancy loss, HC healthy control, GO gene ontology, KEGG kyoto encyclopedia of genes and genomes, PBMC human peripheral blood mononuclear cell. The P value was obtained by two-tailed unpaired Student's t-test (**I, J**), and data are presented as mean ± SD. Source data are provided as a Source Data file.

(Supplementary Fig. 2D–G), only the level of CD107a and IFN-γ in the EPL group showed a statistically significant increase compared to the HC group, further underscoring the functional specificity of dysregulated CD11c + CD8 + T cells in EPL residing in the decidua.

Changes in early gestational maternal serum profiles of cytokines and cytotoxic molecules profiles related to CD11c + CD8 + T cells in EPL

Based on the aforementioned findings, we further explored the expression of cytokines and cytotoxic molecules related to CD11c + CD8 + T cell function in serum from women at 4–5 weeks of gestation, derived from 32 HC and 32 EPL patients. Supplementary Table 1 shows that there are no statistically significant differences between the EPL group and the HC group in terms of age, body mass index (BMI), duration of infertility, type of infertility, anti-Müllerian hormone (AMH), basal follicle-stimulating hormone (FSH), luteinizing hormone (LH), estradiol, progesterone, testosterone, prolactin, thyroid-stimulating hormone (TSH), and bilateral antral follicle count (AFC), indicating that the baseline characteristics of the two groups are comparable. A heatmap was generated to visualize the overall expression profiles of these molecules in the two groups (Supplementary Fig. 3A). PCA distribution plots show the spatial classification of samples between the two groups (Supplementary Fig. 3B). The violin plots reveal that levels of IL-17A, IFN-γ, perforin, and granulysin in the EPL group are significantly higher than those in the HC group ($P < 0.05$). Additionally, compared to the HC group, levels of IL-2, Fas, Granzyme A, and Granzyme B exhibited an increasing trend, though the differences were not statistically significant ($P > 0.05$) (Fig. 3A). Detailed serum levels of the twelve molecules in both groups are summarized in Table 1. The variations in the cytokine and cytotoxic molecule profiles associated with CD11c + CD8 + T cells in maternal serum may influence pregnancy outcomes by modulating immune responses.

To assess the potential of these differentially expressed serum biomarkers in predicting EPL occurrence, we plotted receiver operating characteristic (ROC) curves for each biomarker (Fig. 3B). The results indicate that these serum biomarkers have moderate predictive value, with the area under the curve (AUC) values as follows: IL-2 (0.58), IL-4 (0.50), IL-6 (0.54), IL-10 (0.58), IL-17A (0.67), IFN-γ (0.73), Fas (0.58), FasL (0.54), Granzyme A (0.50), Granzyme B (0.61), perforin (0.75), and granulysin (0.65). We then performed a combined modeling analysis using logistic regression (LR) with IL-17A, IFN-γ, perforin, and granulysin, which were differentially expressed and performed well in the ROC curves, to predict EPL occurrence (Fig. 3C). The combined model achieved an AUC of 0.95 (95% CI: 0.89-1.00, $P < 0.0001$), with a sensitivity of 81.25% and specificity of 96.88%, indicating that this model is highly effective in predicting EPL. Additionally, using machine learning, we evaluated five different EPL prediction models based on IL-17A, IFN-γ, perforin, and granulysin, including K-Nearest Neighbors (KNN), LR, Support Vector Machine (SVM), Random Forest (RF) and eXtreme Gradient Boosting (XGBoost). The dataset of 64 samples was randomly divided into a training set ($n = 32$) and a testing set ($n = 32$) using a 1:1 ratio. The results showed that the LR model demonstrated robust predictive performance, achieving AUCs of 0.95 (95% CI: 0.85-1.00, $P < 0.0001$) for the train set (Supplementary Fig. 3C) and 0.95 (95% CI: 0.81–1.00, $P < 0.0001$) for the test set (Supplementary Fig. 3D). This further supports the important association between dysregulated cytokines and cytotoxic molecules related to CD11c + CD8 + T cell function in early gestational maternal serum and the risk of EPL.

Cytotoxic CD11c + CD8 + T cells inhibit trophoblast invasion via NLRP3/Caspase-1/GSDMD-mediated pyroptosis

To further investigate the roles of altered frequency and function of CD11c + CD8 + T cells in EPL development, we first sorted CD8 + T cells from the decidual tissue of 3 HC women and 3 EPL patients, respectively. Due to the limited availability of human decidua, we were unable to enrich sufficient primary CD11c + CD8 + T cells for in vitro experiments; therefore, we opted to isolate CD8 + T cells and co-cultured them with HTR-8/SVneo trophoblasts using a contact-independent co-culture system (Fig. 4A). The decidual CD8 + T cells and HTR-8/SVneo trophoblasts were seeded in the upper and lower chambers of cell culture inserts, respectively, at a 1:1 ratio, allowing interactions primarily through soluble factors such as cytokines rather than direct cell-to-cell contact. Representative flow cytometry gating plots for decidual CD8 + T cells are shown in Fig. 4B. Given that the sequencing analysis revealed significant enrichment of genes and pathways related to inflammatory cell death in CD11c + CD8 + T cells, we examined the expression levels of pyroptosis-related proteins in HTR-8/SVneo trophoblasts after co-culture, including NLRP3, Caspase-1, and GSDMD. The results showed that decidual CD8 + T cells from the EPL group significantly induced the expression of NLRP3, Caspase-1, and GSDMD in trophoblasts, while HC group-derived cells did not. MCC950, a potent and selective NLRP3 inhibitor, is widely used to inhibit NLRP3 inflammasome activation-mediated pyroptosis[29]. Notably, pre-treatment with MCC950 partially rescued this upregulation (Fig. 4C). Functional assays further demonstrated that decidual CD8 + T cells from the EPL group markedly inhibited trophoblast invasion (Fig. 4D) and placental organoid formation (Fig. 4E) compared to both the blank control and the HC group. Supplementary Fig. 4A shows that the placental organoids were verified through cytokeratin 7 (CK7) and F-actin immunofluorescence staining. Similarly, MCC950 pre-treatment partially alleviated these inhibitory effects. These findings suggest that NLRP3/Caspase-1/GSDMD-mediated pyroptosis may be involved in the observed reduction of trophoblast invasion. Furthermore, flow cytometry analysis of the co-cultured CD8 + T cells showed that the EPL group exhibited a significantly increased frequency of CD11c + CD8 + T cells (Supplementary Fig. 4B) and markedly elevated levels of CD107a, granzyme B, perforin, IFN-γ and TNF-α compared to the HC group (Supplementary Fig. 4C).

Additionally, we further sorted CD11c + CD8 + T and CD11c- CD8 + T cell populations from the peripheral blood of five healthy early

https://doi.org/10.1038/s41467-025-61992-8

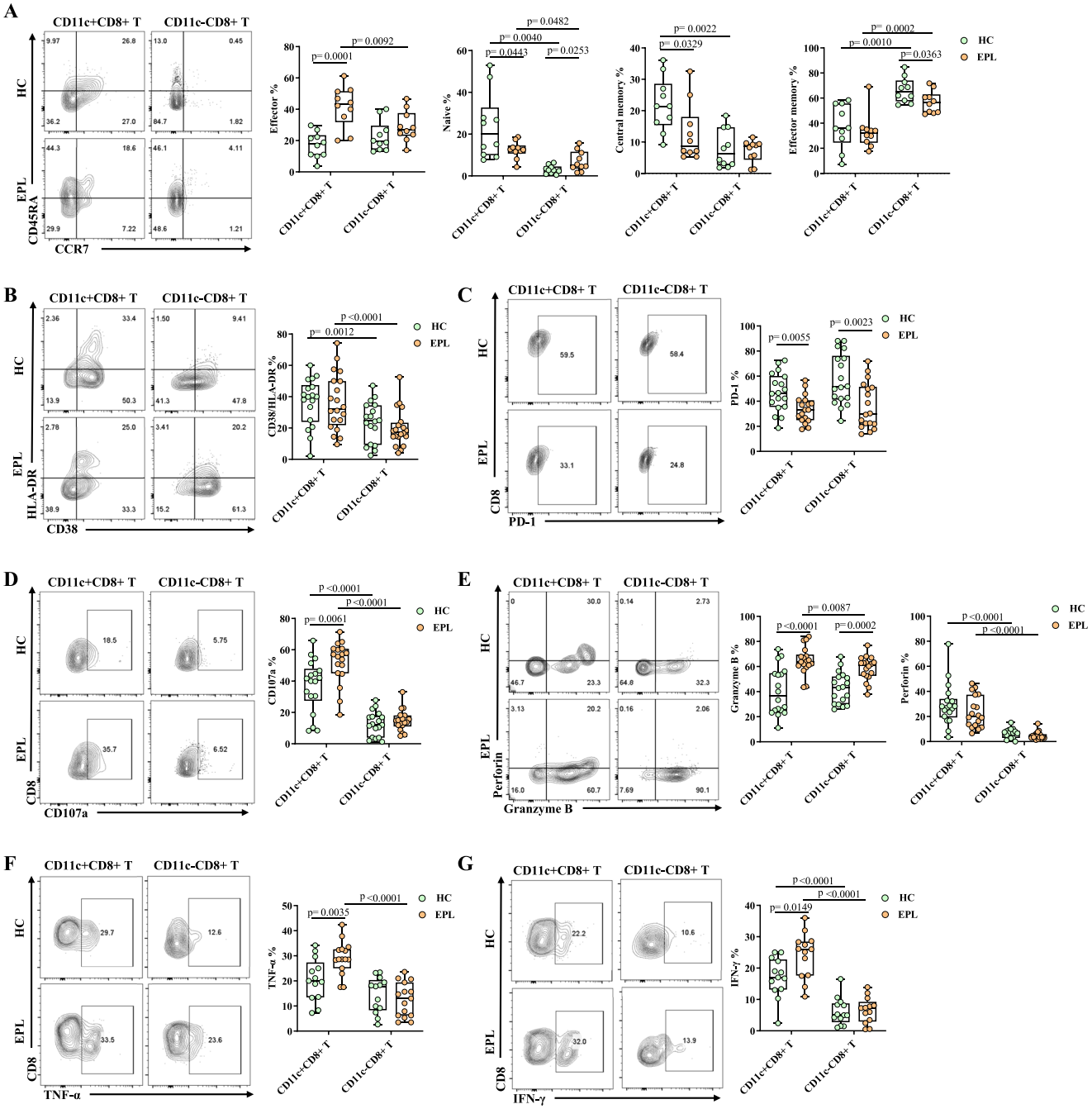

Fig. 2 | Phenotypic and functional characteristics of decidual CD11c + CD8 + T cells in EPL patients. A Subpopulation distribution of decidual CD8 + T cells in HC ($n = 10$) and EPL ($n = 10$) patients, with a typical flow cytometry plot shown on the left. **B** Proportion of CD38 and HLA-DR double-positive subset within decidual CD8 + T cells from HC ($n = 18$) and EPL ($n = 20$) patients. **C** Proportion of PD-1 expression on decidual CD8 + T cells from HC ($n = 18$) and EPL ($n = 18$) patients. **D** Expression of CD107a on decidual CD8 + T cells from HC ($n = 18$) and EPL ($n = 18$) patients. **E** Expression of granzyme B and perforin in decidual CD8 + T cells from HC ($n = 18$) and EPL ($n = 18$) patients. **F** Secretion of TNF-α from decidual CD8 + T cells in HC ($n = 13$) and EPL ($n = 13$) patients. **F, G** Secretion of IFN-γ from decidual CD8 + T cells in HC ($n = 13$) and EPL ($n = 13$) patients. EPL early pregnancy loss, HC healthy control. The P value was obtained by two-tailed unpaired Student's t-test (**A**–**G**), and data are presented as mean ± SD. Source data are provided as a Source Data file.

pregnant women using flow cytometry and then co-cultured them with HTR-8/SVneo immortalized human trophoblast cells (Supplementary Fig. 5A). Representative flow cytometry gating plots are shown in Supplementary Fig. 5B. Transwell invasion assays revealed that peripheral blood CD11c + CD8 + T cells significantly inhibited the invasion capacity of HTR-8/SVneo trophoblasts compared to the CD11c-CD8 + T group (Supplementary Fig. 5C). Flow cytometry detection of the two cell populations after co-culture showed that CD11c + CD8 + T cells were enriched primarily in the effector cell subpopulation, with increased HLA-DR expression, decreased PD-1 expression, and a higher capacity than CD11c-CD8 + T cells to secrete CD107a, granzyme B, perforin, IFN-γ and TNF-α (Supplementary Fig. 5D–G).

IFN-γ has been reported to mediate tumor cell pyroptosis[30,31]. To further investigate the potential mediation role of IFN-γ in CD11c + CD8 + T cell-induced trophoblast pyroptosis, we utilized HTR-8/SVneo trophoblasts and primary EVT cells isolated from early pregnancy chorionic tissue to model the effects of increased IFN-γ expression in vitro. Evidence of pyroptosis was examined through the expression

https://doi.org/10.1038/s41467-025-61992-8

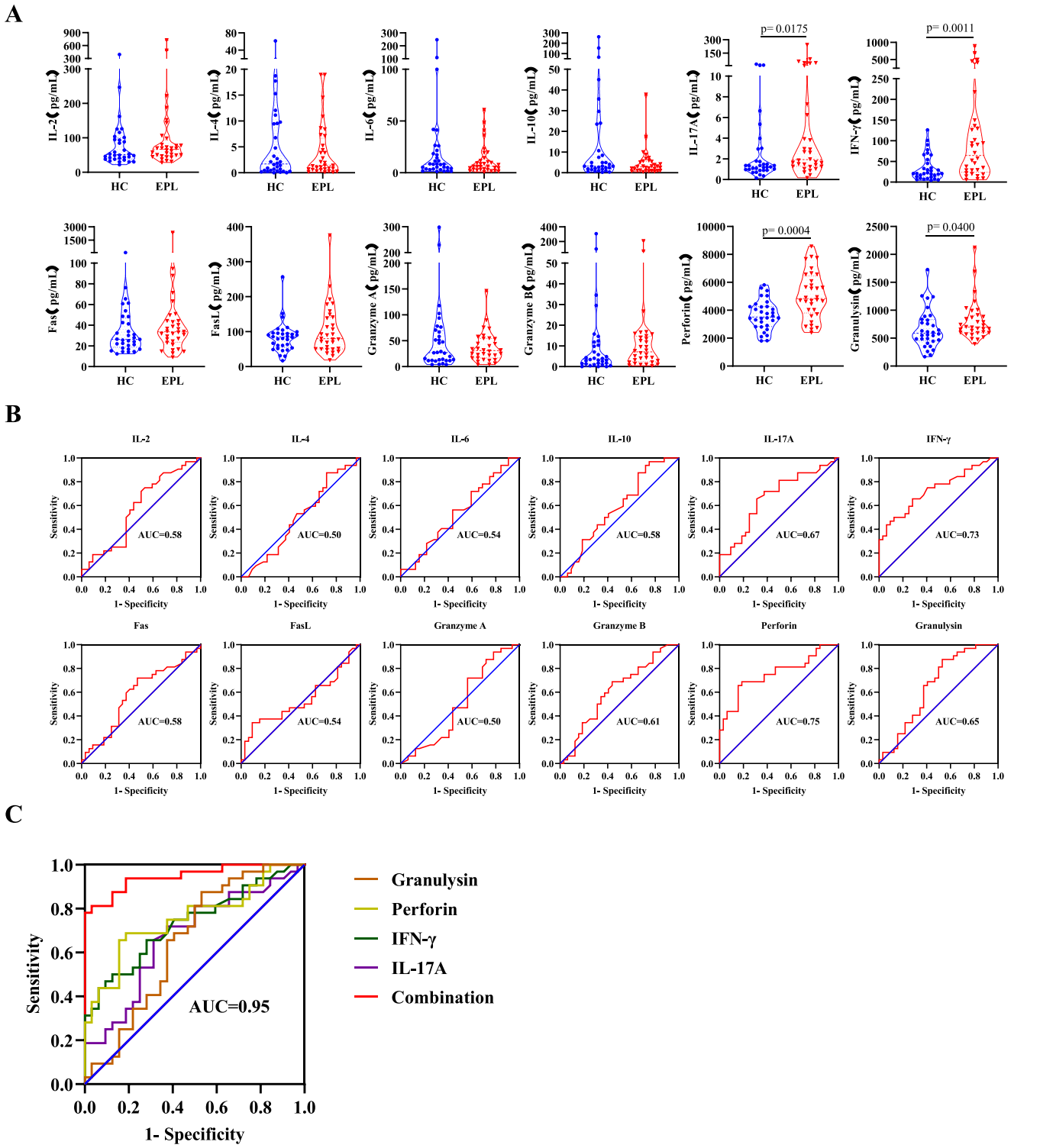

Fig. 3 | Alterations in immune-related cytokine and cytotoxic molecule expression profiles in early pregnancy serum of EPL patients. A Violin plots displaying the distribution of 12 serum biomarkers in the HC group ($n = 32$) and the EPL group ($n = 32$). The P value was obtained by the Mann-Whitney U test (**A**), and data are presented as median with interquartile range. **B** ROC curves showing the performance of the 12 serum biomarkers in predicting EPL risk. **C** ROC curves of a combined prediction model using the top four differentially expressed serum biomarkers (IL-17A, IFN-γ, perforin, and granulysin). The combined model achieved an AUC of 0.95 (95% CI: 0.89-1.00, $P < 0.0001$), with a sensitivity of 81.25% and specificity of 96.88%. P value was calculated using DeLong's two-sided test for ROC curve comparisons. The combination model was derived using logistic regression. EPL early pregnancy loss, HC healthy control, ROC receiver operating characteristic, AUC area under the curve. Source data are provided as a Source Data file.

Table 1 | Serum cytokine and immune molecule expression

Characteristics	EPL group (*N* = 32)	HC group (*N* = 32)	*P* values
IL-2 (pg/mL)	66.84 (47.90–94.24)	51.48 (38.73–99.72)	0.277
IL-4 (pg/mL)	1.44 (0.64–6.69)	1.71 (0.40–9.52)	0.989
IL-6 (pg/mL)	6.30 (3.21–13.82)	8.28 (3.68–20.82)	0.568
IL-10 (pg/mL)	2.82 (1.11–5.60)	3.16 (1.78–20.29)	0.251
IL-17A (pg/mL)	1.93 (1.28–7.04)	1.28 (0.92–2.67)	0.018
IFN-γ (pg/mL)	64.45 (23.74–134.78)	20.66 (12.46–52.17)	0.001
Fas (pg/mL)	33.63 (23.60–44.36)	26.37 (18.60–46.92)	0.262
FasL (pg/mL)	79.75 (50.68–140.96)	84.84 (55.26–95.93)	0.629
Granzyme A (pg/mL)	30.95 (16.80–54.47)	27.03 (11.72–69.69)	0.979
Granzyme B (pg/mL)	7.15 (2.36–14.71)	3.67 (1.36–11.48)	0.133
Perforin (pg/mL)	4834.37 (3805.18–6452.29)	3514.57 (2839.23–4261.79)	<0.001
Granulysin (pg/mL)	699.65 (599.53–908.69)	589.16 (450.08–832.18)	0.040

The P value was obtained by the Mann-Whitney U test, and data are presented as median with interquartile range. $P < 0.05$ was considered statistically significant. *IL* interleukin, *IFN-γ* interferon-γ, *TNF-α* tumor necrosis factor-α,*EPL* early pregnancy loss, *HC* healthy control.

levels of pyroptosis-related genes and proteins, propidium iodide (PI) fluorescence staining and electron microscopy. Our findings indicated that treatment of HTR-8/SVneo trophoblasts with exogenous recombinant IFN-γ significantly increased the expression of NLRP3, Caspase-1, and GSDMD (Fig. 5A, B). We found that, compared to the control and MCC950-pretreated groups, the IFN-γ-treated group exhibited a significantly higher proportion of PI-positive pyroptotic cells (Fig. 5C). Moreover, transwell invasion and wound healing assays demonstrated that the IFN-γ-treated group significantly impaired the invasion and migration abilities of trophoblasts compared to the control and MCC950-pretreated groups (Fig. 5D, E). Additionally, IFN-γ treatment markedly reduced primary EVT migration and outgrowth sprouting from the villous tips of explants (Fig. 5F).

The purification of primary EVT cells used in our study were validated by immunofluorescence co-staining with trophoblast- and EVT-specific markers CK7 and human leukocyte antigen-G (HLA-G) (Fig. 6A). Subsequent PI staining revealed that the proportion of PI-positive EVT cells in the IFN-γ treatment group was significantly higher compared to the control and MCC950-pretreated groups (Fig. 6B). Scanning electron microscopy revealed that EVT cell membranes in the IFN-γ treatment group displayed prominent signs of pyroptosis, such as rupture and perforation (Fig. 6C). Transwell invasion and wound healing assays also revealed that IFN-γ treatment significantly inhibited the invasion and migration abilities of EVT cells compared to the control and MCC950-pretreated groups, consistent with the findings from HTR-8/SVneo cells (Fig. 6D, E). These results support that the enrichment of decidual CD11c + CD8 + T cells in EPL patients impairs trophoblast biological behavior through the secretion of cytotoxic molecules and cytokines, particularly IFN-γ, which activates NLRP3/Caspase-1/GSDMD-mediated pyroptosis, ultimately leading to pregnancy loss.

4-1BB-induced enrichment and activation of CD11c + CD8 + T cells lead to abortion in mice

To confirm the role of CD11c + CD8 + T cells in pregnancy loss in vivo, we applied a classic spontaneous abortion mouse model. The abortion-prone (AP) group consisted of CBA/J female mice mated with DBA/2 J male mice, while the normal pregnancy (NP) group included CBA/J female mice mated with BALB/c male mice. As the immune costimulatory molecule 4-1BB, a member of the tumor necrosis factor receptor superfamily, is expressed on the surface of activated CD8 + T cells[32,33] and promotes the proliferation and differentiation of CD11c + CD8 + T cells[34], we used agonistic anti-4-1BB antibodies to induce their activation. Pregnant mice in the NP group were injected with these antibodies to construct a model with upregulated CD11c + CD8 + T cell expression and functional activation (4-1BB group) (Fig. 7A). Compared to the NP group, the AP group showed a significant decrease in the number of live fetuses *per* pregnant mouse and a significantly higher rate of embryo resorption, approximately 40% (Fig. 7B–C), which roughly equals to the reported abortion rate of this model[35]. Similar to the findings in the AP group, the 4-1BB group presented significant embryo resorption compared to the NP group (Fig. 7B–C). Additionally, there was no significant difference in the body weight of pregnant mice at E12.5 among the three groups (Fig. 7D).

Next, we verified the phenotypic and functional changes of CD11c + CD8 + T cells in the abortion mouse model. As shown in Supplementary Fig. 6, the gating strategy for CD8 + T cells was applied to mouse decidua, spleen, and peripheral blood. Similar to our findings in human studies, CD11c + CD8 + T cells were specifically enriched in the decidua of NP mice compared to those in peripheral blood and spleen (Supplementary Fig. 7A). Compared with those in the NP group, the proportions of CD11c + CD8 + T cells in the decidua in the AP and 4-1BB groups were significantly greater (Fig. 7E). In addition, the expression of CD69, CD107a, granzyme B, perforin, and IFN-γ in decidual CD11c + CD8 + T cells was increased by varying degrees in the AP and 4-1BB groups when compared with the NP group (Fig. 7F, G). Similar trends were also observed in the peripheral blood and spleen tissues (Supplementary Fig. 7B–G). These results further indicate that, similar to EPL patients, the proportion of decidual CD11c + CD8 + T cells is significantly increased in spontaneous abortion mice. Thus, these cells may participate in the abortion phenotype by secreting specific cytotoxic molecules and cytokines. Additionally, we observed the structure of the pregnant uterus in the three groups of mice using HE staining and analyzed the depth of CK7+ trophoblast cell infiltration into the uterine decidua through immunofluorescence staining. The results showed that, compared to the NP group, the depth of CK7+ trophoblast cell infiltration into the decidua was significantly reduced in the AP and 4-1BB groups (Fig. 7H–I). Meanwhile, immunofluorescence staining of the placental tissue revealed that, compared to the NP group, the expression of pyroptosis-related proteins was increased in the AP and 4-1BB groups (Supplementary Fig. 7H). These findings suggest that decidual CD11c + CD8 + T cells contribute to pregnancy loss by impairing normal trophoblast behaviors, highlighting the importance of cross-talk between CD8 + T cells and trophoblasts at the maternal-fetal interface in the establishment and maintenance of pregnancy.

Discussion

Several studies have shown abnormalities in the local immune microenvironment of EPL, particularly involving altered CD8 + T cell subsets and an imbalance between pro-inflammatory and anti-inflammatory signals[15,36]. The specific characterization of abnormally activated CD8 + T cell subsets in EPL has been lacking, however. In this study, we identified significant activation and enrichment of cytotoxic CD11c + CD8 + T cells in the decidua and peripheral blood of EPL patients for the first time, while detailing their phenotypic and functional characteristics. We also developed an effective multi-biomarker predictive model for EPL based on functional cytokines and cytotoxic molecules associated with CD11c + CD8 + T cells in early gestational maternal serum. Notably, we found that CD11c + CD8 + T cells inhibit trophoblast invasion through IFN-γ, indicating a dysregulated maternal-fetal cellular cross-talk at the maternal-fetal interface during EPL development, as illustrated in Fig. 8. Furthermore, we demonstrated that activation of this cell population can induce an abortion phenotype in a mouse model. These findings underscore the previously unrecognized role of CD11c + CD8 + T cells at the maternal-fetal

https://doi.org/10.1038/s41467-025-61992-8

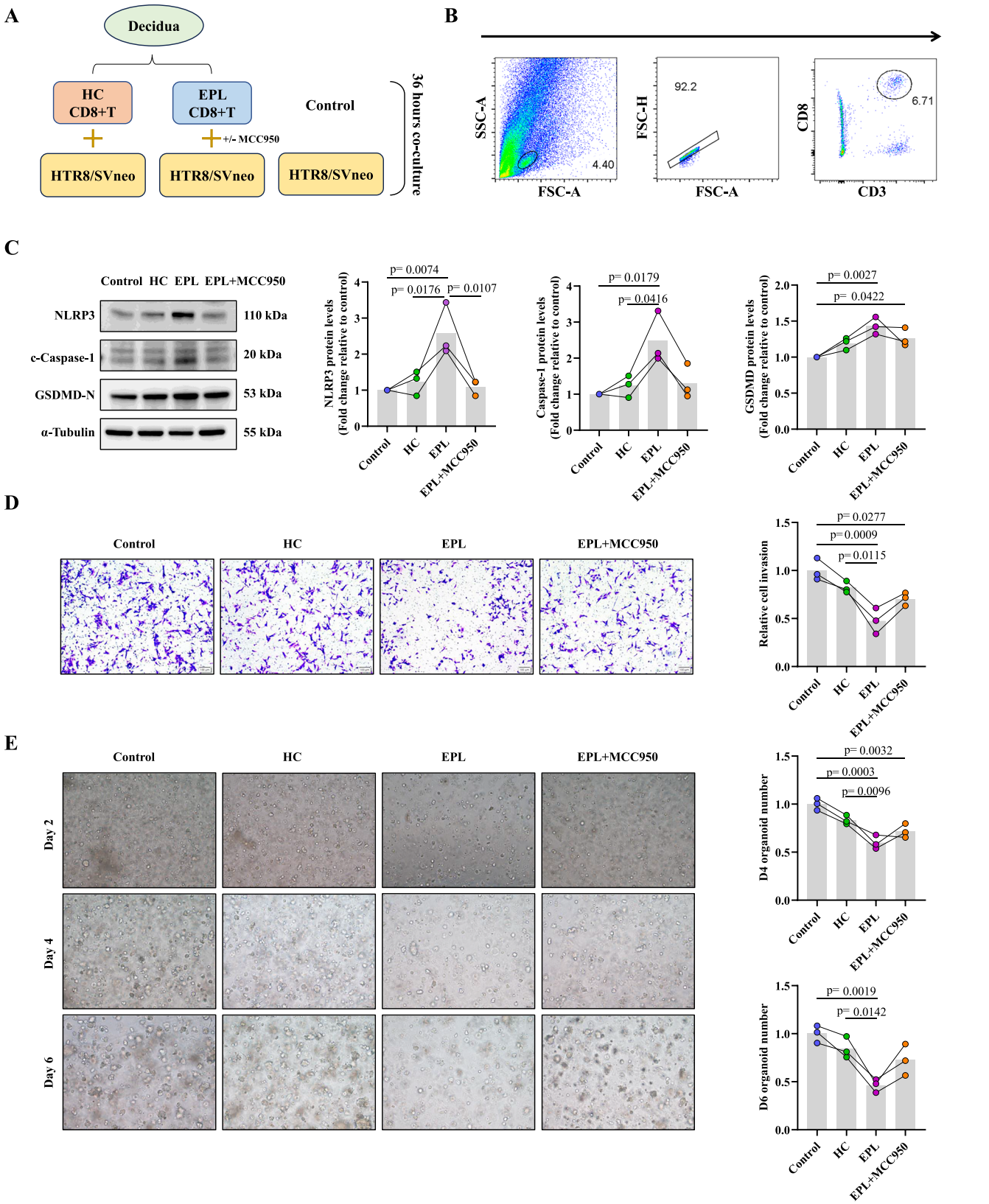

Fig. 4 | Inhibition of trophoblast invasion by decidual CD11c + CD8 + T cells from EPL patients via NLRP3/Caspase-1/GSDMD-mediated pyroptosis. **A** Schematic representation of sorting CD8 + T cells from EPL and HC decidua and their in vitro co-culture experiment with HTR-8/SVneo trophoblasts. **B** Typical flow cytometry gating strategy for sorting CD8 + T cells from human decidua. **C** Western blotting examining the impact of human decidual CD8 + T cells on protein levels of NLRP3, Caspase-1, and GSDMD in HTR-8/SVneo trophoblasts ($n = 3$ biologically independent experiments). **D** Transwell assays assessing the effect of human decidual CD8 + T cells on HTR-8/SVneo trophoblast invasion capabilities ($n = 3$ biologically independent experiments). Scale bar = 100 μm. **E** Quantification and representative images of placental organoid formation in the presence of human decidual CD8 + T cells ($n = 3$ biologically independent experiments). Scale bar = 100 μm. EPL early pregnancy loss, HC healthy control. The P value was obtained by one-way ANOVA (**C**–**E**), and data are presented as mean ± SD. Source data are provided as a Source Data file.

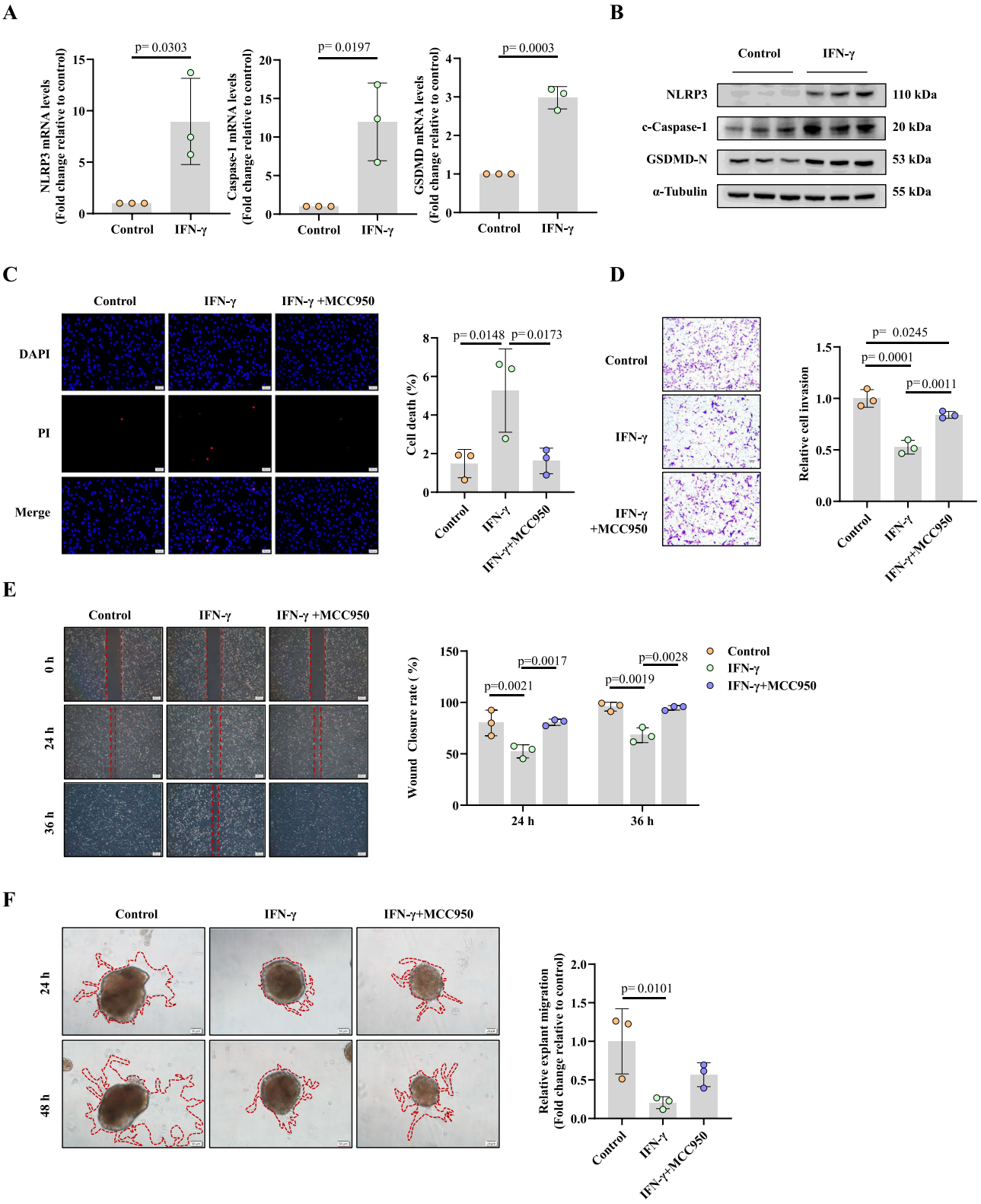

interface, offering targets for therapeutic intervention and enhancing predictive capabilities for EPL management.

Extensive research has highlighted the cytotoxic role of CD11c in CD8 + T cells, particularly in contexts such as antiviral immunity, cancer, and autoimmune diseases. Notably, high CD11c expression in CD8 + T cells has been associated with potent anti-tumor effects in models of colorectal cancer and lymphoma[17,37]. Similarly, during infections like human immunodeficiency virus and hepatitis B, virus-specific CD8 + T cells with elevated CD11c levels secrete increased amounts of cytotoxic markers, including granzyme B and perforin, alongside pro-inflammatory cytokines like IFN-γ and TNF-α[18,38]. In our study, we observed a significant increase of CD11c + CD8 + T cells in EPL patients, predominantly within the effector cell subset. These CD11c + CD8 + T cells exhibited heightened expression of activation markers, such as CD38 and HLA-DR, suggesting a state of excessive activation. Interestingly, despite the common association of CD8 + T

Fig. 5 | IFN-γ modulates HTR-8/SVneo trophoblast behavior by inducing pyroptosis via activation of the NLRP3/Caspase-1/GSDMD pathway. A, B HTR-8/SVneo trophoblasts were treated with or without IFN-γ (10 ng/ml), and qPCR and western blotting were used to detect the mRNA (**A**) and protein (**B**) expression levels of NLRP3, Caspase-1, and GSDMD in HTR-8/SVneo trophoblasts ($n = 3$ biologically independent experiments). **C** PI staining shows the proportion of PI-positive (red) cells in HTR-8/SVneo trophoblasts treated with or without IFN-γ (10 ng/ml) alone, or pretreated with MCC950 (10 μM) for 1 hour before IFN-γ treatment ($n = 3$ biologically independent experiments). Scale bar = 100 μm. **D, E** Transwell and wound healing assays were performed to evaluate the effects of with or without IFN-γ (10 ng/ml) treatment alone, or pre-treatment with MCC950 (10 μM) for 1 hour before IFN-γ treatment, on the invasion (**D**) and migration (**E**) capabilities of HTR-8/SVneo trophoblasts ($n = 3$ biologically independent experiments). Scale bar = 100 μm (**D**), 200 μm (**E**). **F** After 24 hours of in vitro culture, human villous explants were treated with or without IFN-γ (10 ng/ml) or pretreated with MCC950 (10 μM) for 1 hour before IFN-γ treatment. The outward growth of EVT from the explants (outlined in red) was assessed at 48 hours ($n = 3$ biologically independent experiments). Scale bar = 50 μm. qPCR quantitative polymerase chain reaction, PI propidium iodide, EVT extravillous trophoblast. The P value was obtained by two-tailed unpaired Student's t-test (**A**), one-way ANOVA (**C**–**F**), and data are presented as mean ± SD. Source data are provided as a Source Data file.

cell exhaustion in tumors, EPL patients displayed a decrease in the exhaustion marker PD-1, indicating that these cells may retain a more functional phenotype.

This observation aligns with previous findings that CD11c + CD8 + T cells represent a highly activated, minimally exhausted subset, potentially endowing them with enhanced effector functions[18]. Consistent with this, CD11c + CD8 + T cells expressed higher levels of granzyme B, perforin, and CD107a, and secreted greater amounts of IFN-γ and TNF-α compared to their CD11c- counterparts. Notably, CD11c + CD8 + T cells in the decidua of EPL patients released significantly more cytokines and cytotoxic molecules than those in control participants. The significant enrichment of CD11c + CD8 + T cells in the decidua compared to PBMCs, suggests that their activation and recruitment may be driven by the local immune microenvironment at the maternal-fetal interface. We speculate that factors such as cytokines, chemokines, or other immune regulatory molecules within the decidua, as well as potential antigenic stimulation from embryonic-derived antigens, may contribute to the local recruitment and activation of these cells. These findings suggest that CD11c + CD8 + T cells may play a role in attacking the fetus similarly to how they target tumors or infections, contributing to EPL through their potent effector functions. This raises important questions about the balance between immune activation and tolerance during pregnancy, as heightened cytotoxic responses could inadvertently compromise fetal viability.

The complexity of the etiological mechanisms behind EPL has led to limited research on predictive models. This highlights the urgent need for accurate tools to identify high-risk individuals early and facilitate targeted interventions. Current models primarily rely on clinical features and imaging data, which often lack sufficient sensitivity and specificity[39,40]. Studies have shown that the risk of adverse pregnancy outcomes is significantly higher in individuals who conceive following IVF-ET compared to those with natural conception[41]. Building on our findings regarding the role of CD11c + CD8 + T cells in maintaining maternal-fetal immune homeostasis, we investigated various cytokines and cytotoxic molecules associated with these cells in early pregnancy serum from IVF-ET cohorts. Notably, we identified significant differences in levels of cytokines such as IL-17A, IFN-γ, perforin, and granulysin between the EPL and HC groups. By combining these altered biomarkers, we developed a robust early prediction model for EPL. These findings suggest that the cytokines and cytotoxic molecules associated with CD11c + CD8 + T cells may serve as potential candidates for early clinical screening and intervention. Future studies should include longitudinal tracking with multiple serum samples across different pregnancy stages to optimize and validate the predictive model's applicability. Importantly, differences in immune status between IVF-ET and naturally conceived pregnancies may introduce variability in biomarker expression. While IVF-ET pregnancies offer a well-defined clinical setting for standardized sampling and model development, future studies should incorporate validation in natural pregnancy cohorts to enhance the model's generalizability and clinical relevance.

It is crucial to recognize that many of these cytokines and cytotoxic molecules are not only associated with CD11c + CD8 + T cells but also play a pivotal role in NK cell function, particularly within the decidual microenvironment. Decidual NK (dNK) cells serve as key regulators in early pregnancy, contributing to immune tolerance at the maternal-fetal interface. Studies have shown that dNK cell dysfunction is closely linked to pregnancy complications such as recurrent pregnancy loss[42,43]. Essential cytotoxic molecules, including perforin and granzyme B, mediate NK cell function by inducing apoptosis in target cells[44,45], while inflammatory cytokines such as IFN-γ and TNF-α, when aberrantly expressed, can trigger excessive inflammatory responses, potentially compromising normal embryonic development[44,46]. Moreover, interactions between dNK cells and other cells, including macrophages[47] and stromal cells[48], may further shape the immune landscape at the maternal-fetal interface. Given the overlapping roles of CD11c + CD8 + T cells and NK cells in immune regulation, future research should focus on uncovering potential synergistic mechanisms between these cell populations in the pathogenesis of EPL, aiming to refine predictive models and develop targeted therapeutic strategies.

Research has shown that key proteins and cytokines produced by T cells may directly influence the growth and biological functions of trophoblast cells or activate macrophages to attack trophoblast cells through pathways involving IFN-γ, TNF-α, TGF-β, and IL-6 receptors, leading to pregnancy loss[15,49,50]. While IFN-γ is known to induce pyroptosis in infectious and autoinflammatory diseases via STAT1 activation[51,52], its impact on trophoblast has been underexplored. Additionally, several recent studies have confirmed that epigenetic modification enzymes, mitochondrial energy metabolism-related proteins, and neutrophil aggregation can induce inflammation and mediate trophoblast pyroptosis, thereby impairing placental function[53–56]. Here, we reveal that IFN-γ induces trophoblast pyroptosis by activating the classic NLRP3/Caspase-1/GSDMD pathway, thereby impairing their invasion, migration, and ability to grow outward from the explant. These results highlight the potential role of IFN-γ in trophoblast pyroptosis and suggest that CD11c + CD8 + T cells may disrupt immune balance at the maternal-fetal interface while also modulating trophoblast behavior, contributing to EPL development.

Furthermore, CD11c + CD8 + T cells have been associated with infections, colorectal cancer, and melanoma treatment[34,57,58]; however, there are currently no reported inhibitors targeting these cells. Notably, 4-1BB agonists can induce antigen-specific differentiation and expansion of CD11c + CD8 + T cells. Leveraging the immunostimulatory properties of 4-1BB, we designed an in vivo mouse model that upregulates the expression and functional activation of CD11c + CD8 + T cells during early pregnancy. Our results indicated that mice exposed to 4-1BB exhibited an increased proportion of CD11c + CD8 + T cells, enhanced secretion of cytotoxic molecules and cytokines, and significant embryonic loss, along with impaired trophoblast invasion into the decidua, mirroring observations in AP mouse models. However, it is important to note that trophoblast invasion in the murine placenta is inherently less extensive than in

https://doi.org/10.1038/s41467-025-61992-8

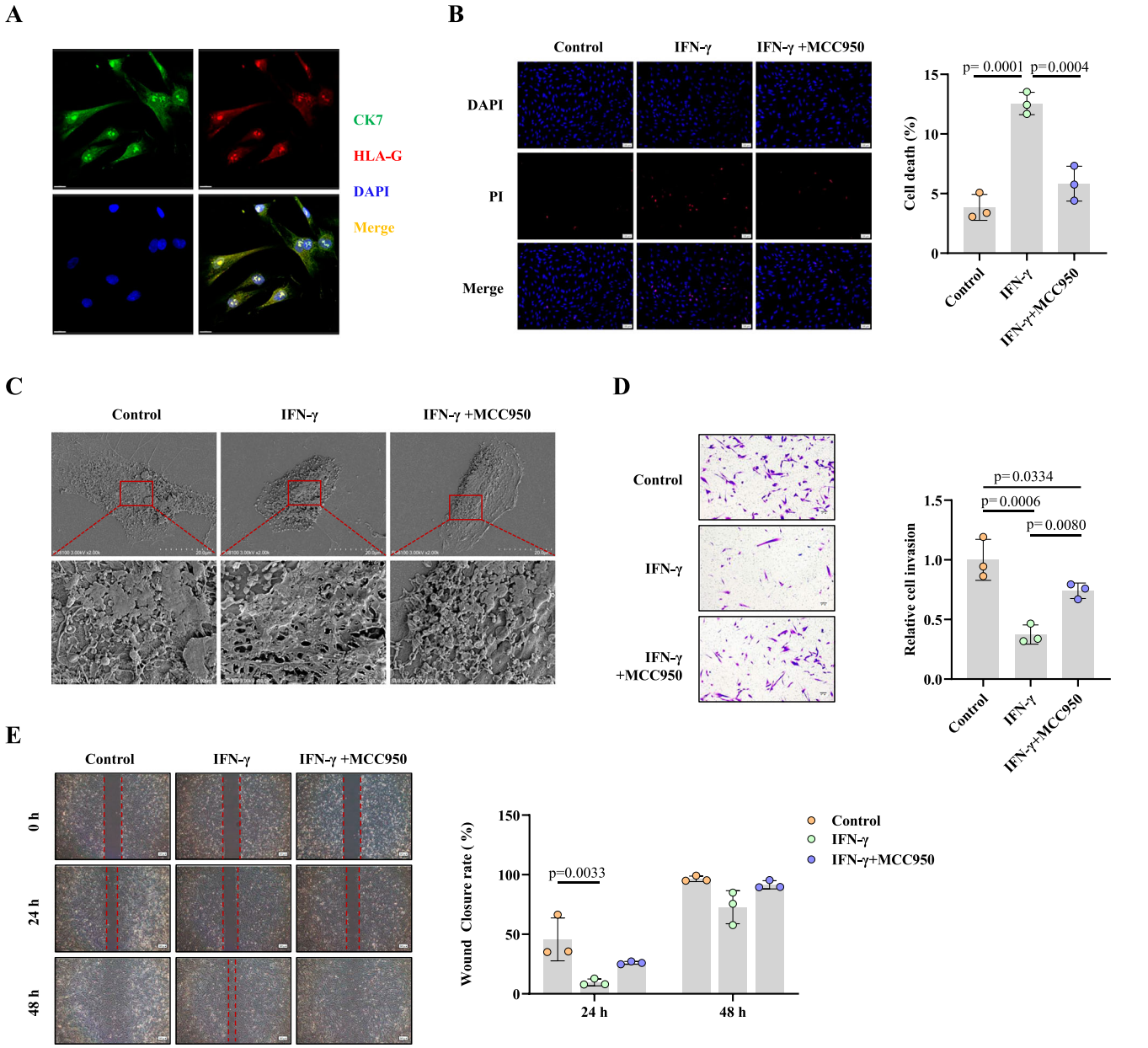

Fig. 6 | IFN-γ induces pyroptosis in human primary EVT cells, leading to reduced invasion and migration. A Immunofluorescence staining for CK7 (green) and HLA-G (red) was used to verify the purity of human primary EVT cells. Scale bar = 20 μm. Representative results from three independent biological replicates. **B** PI staining shows the proportion of PI-positive (red) cells in human primary EVT cells treated with or without IFN-γ (10 ng/ml) alone, or pretreated with MCC950 (10 μM) for 1 hour before IFN-γ treatment ($n = 3$ biologically independent experiments). Scale bar = 100 μm. **C** Scanning electron microscopy reveals the cell morphology of human primary EVT cells with or without IFN-γ (10 ng/ml) treatment, or pretreated with MCC950 (10 μM) for 1 hour before IFN-γ treatment. Scale bar = 20 μm. Representative results from three independent biological replicates. **D, E** Transwell and wound healing assays were conducted to assess the effects of with or without IFN-γ treatment alone, or pretreated with MCC950 (10 μM) for 1 hour before IFN-γ treatment, on the invasion (**D**) and migration (**E**) capabilities of human primary EVT cells ($n = 3$ biologically independent experiments). Scale bar = 100 μm (**D**), 200 μm (**E**). EVT extravillous trophoblast, CK7 cytokeratin 7, HLA-G human leukocyte antigen-G, PI propidium iodide. The P value was obtained by one-way ANOVA (**B, D, E**), and data are presented as mean ± SD. Source data are provided as a Source Data file.

humans, and CK7 staining alone may not fully capture the complexity of trophoblast invasion. Future studies should incorporate additional markers and functional assays to provide a more comprehensive evaluation. Additionally, we acknowledge the limitation that anti-4-1BB treatment may also affect other immune cell subsets, which could indirectly influence pregnancy outcomes, and more specific tools are needed to directly assess the role of CD11c + CD8 + T cells in pregnancy loss. These findings further support our hypothesis that CD11c + CD8 + T cells promote EPL through their specific cytotoxic functions. Ultimately, the exploration of targeted interventions aimed at modulating CD11c + CD8 + T cell activity holds promise for developing therapeutic strategies, particularly when combined with existing treatment modalities, such as various immunomodulators[59,60]. This approach may pave the way for improved management of EPL and enhance our understanding of immune dynamics at the maternal-fetal interface.

This study has several advantages and limitations. First, both groups of participants were early pregnant patients who underwent artificial abortion and were matched for gestational age. This ensured for accurate comparisons between the groups, but also resulted in a

https://doi.org/10.1038/s41467-025-61992-8

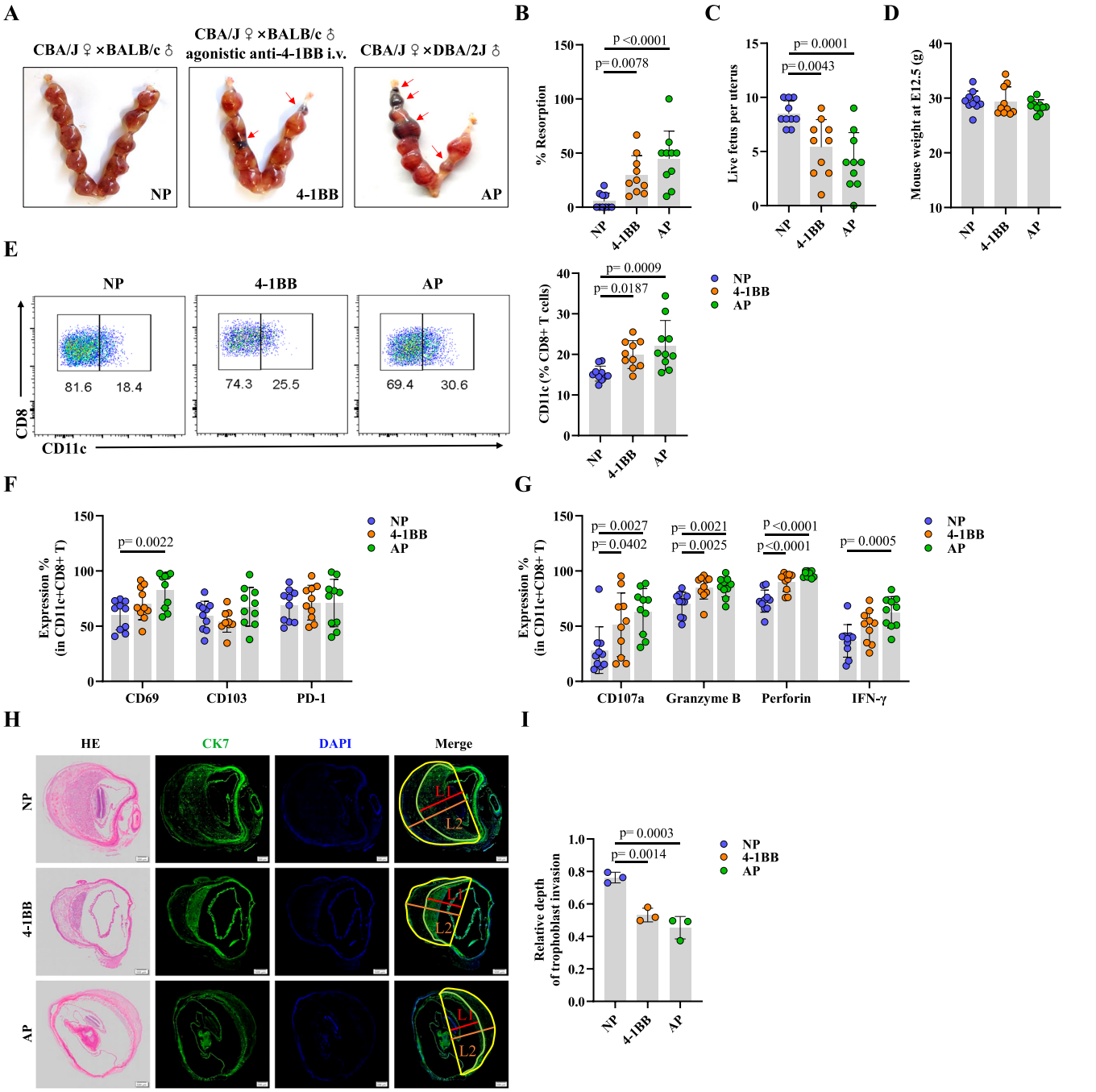

Fig. 7 | Alterations in the frequency and function of CD11c + CD8 + T cells in mice decidua affect early pregnancy maintenance. A Representative images of a pregnant uterus from mice in various groups: NP (normal pregnancy group), 4-1BB (normal pregnant mice injected intravenously with 5 mg/kg anti-mouse 4-1BB antibody at E7.5), and AP (abortion-prone group). **B**–**D** Quantitative statistics of embryo resorption rate (**B**), number of viable embryos per uterus (**C**), and average body weight of pregnant mice at E12.5 (**D**) for each group ($n = 10$). **E** Flow cytometry analysis of CD11c expression in CD8 + T cells isolated from mice decidua in each group ($n = 10$). **F** Expression of CD69, CD103, and PD-1 in CD11c + CD8 + T cells from mice decidua in each group ($n = 10$). **G** Expression of cytotoxicity-related molecules (CD107a, granzyme B, perforin) and cytokine (IFN-γ) in CD11c + CD8 + T cells from mice decidua in each group ($n = 10$). **H** HE and immunofluorescence staining to observe the infiltration depth of CK7+ trophoblast layer (green) into the decidua of mice uterus. The relative depth of EVT infiltration into the uterus is calculated as the ratio of the depth of CK7+ trophoblast layer (L1, red) to the total depth (L2, orange). **I** Quantitative statistics of the relative depth of EVT infiltration into the uterus ($n = 3$ biologically independent experiments). Scale bar = 500 μm. NP normal pregnancy, AP abortion prone, CK7 cytokeratin 7, EVT extravillous trophoblast. The P value was obtained by two-tailed unpaired Student's t-test (**B**–**G, I**), and data are presented as mean ± SD. Source data are provided as a Source Data file.

limited sample size. While the quality of the samples was sufficient, the small sample size may introduce some degree of bias in the study results. Secondly, our study successfully identified a specific subpopulation of CD8 + T cells at the maternal-fetal interface, along with their altered expression and function in EPL. While we have initiated investigations into the interactions between these distinct cells and trophoblasts, further research is needed to elucidate the regulatory mechanisms governing these cells and their interactions with other immune cells at the maternal-fetal interface. Additionally, it is important to note that our in vitro experiments utilized the HTR-8/SVneo cell line, which, despite its widespread use and stability in laboratory settings, has limitations in fully replicating the physiological

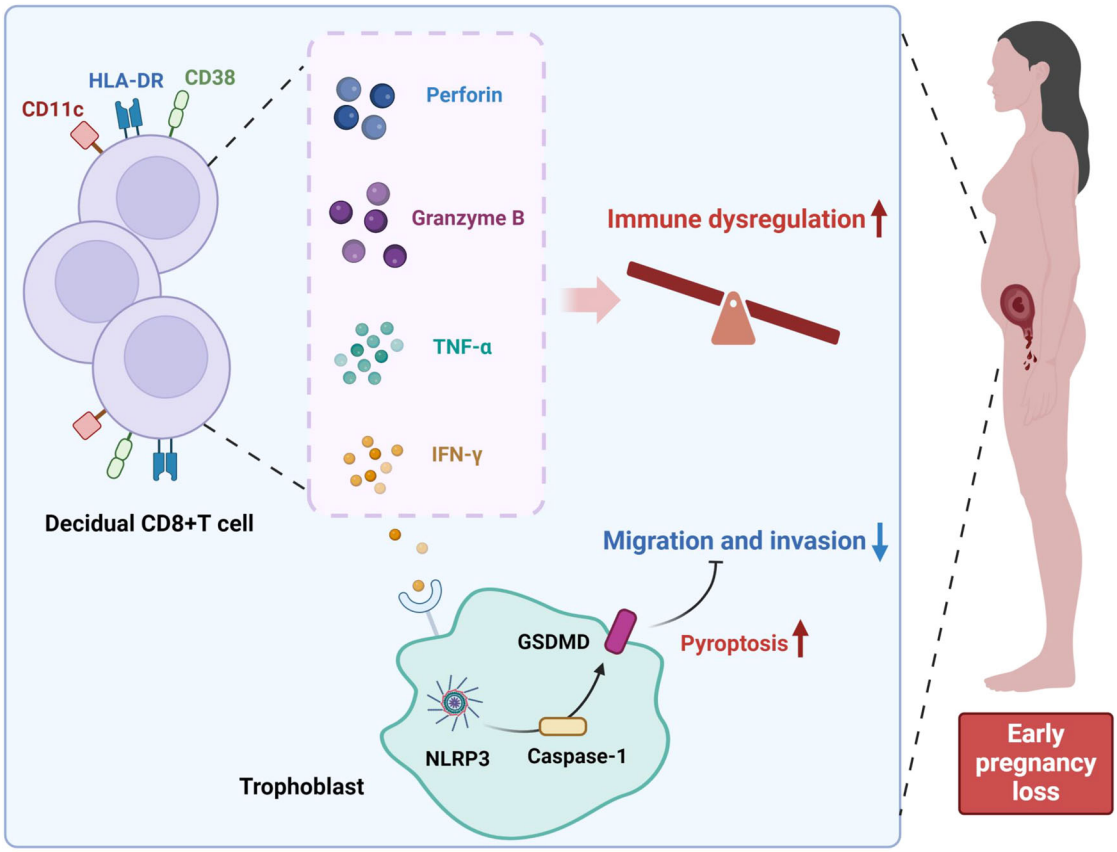

Fig. 8 | Decidual enrichment of CD11c + CD8 + T cells disrupt maternal-fetal immune balance and mediates abnormal trophoblast biological behaviors, leading to EPL. Through the analysis of clinical samples from healthy individuals and EPL patients, as well as in vitro, ex vivo, and in vivo experimental models, we discovered that CD11c + CD8 + T cells are enriched and functionally activated in the decidua of EPL patients, exhibiting potent effector and cytotoxic functions that contribute to immune dysregulation at the maternal-fetal interface. Furthermore, cytokines such as IFN-γ secreted by CD11c + CD8 + T cells in EPL patients can mediate trophoblast pyroptosis, impairing their invasion and migration capabilities, and ultimately leading to EPL. Created in BioRender. Li, Y. (2025) https://BioRender.com/gdpqtyb.

characteristics of primary trophoblasts, particularly in terms of hCG secretion and invasive capacity. The heterologous nature of HTR-8/SVneo cells may also not fully capture the complexity of immune regulation at the maternal-fetal interface. In future studies, we plan to further optimize and expand the use of placental organoids to deepen our understanding of the mechanisms underlying trophoblast dysfunction and immune dysregulation in EPL.

In summary, this study reveals the presence of significantly activated and enriched cytotoxic CD11c + CD8 + T cells in both the decidua and peripheral blood of EPL patients, with the potential to markedly inhibit trophoblast invasion. As a subpopulation, CD11c + CD8 + T cells exhibit altered function at the maternal-fetal interface during early pregnancy, highlighting their pivotal role in EPL pathogenesis. Additionally, we developed a robust early prediction model for EPL based on cytokines and cytotoxic molecules associated with CD11c + CD8 + T cell function. These findings not only provide potential targets for immunotherapies but also offer insights into the development and clinical precision management of EPL.

Methods

Ethics approval

The human and animal experiments in this study were approved by the Ethics Committee of the Center for Reproductive Medicine of Shandong University (Ethical Review No. 116, 2022). In accordance with the Declaration of Helsinki, all participants were informed of the study and signed informed consent forms.

Human samples

This study involved human samples collected from participants recruited at the Reproductive Hospital Affiliated with Shandong University and the Department of Obstetrics and Gynecology, Qilu Hospital of Shandong University, between October 2022 and October 2024. The samples comprised two main components: decidua and PBMCs, along with serum samples from women undergoing IVF-ET.

Decidua and PBMCs were obtained from women who underwent surgical termination of pregnancy between 6-12 weeks of gestation, as described in previous studies[61,62]. The EPL group included women who experienced two or more instances of embryonic arrest or spontaneous abortion with the same partner ($n = 24$), and the samples were collected at the time of pregnancy termination due to embryonic arrest or spontaneous abortion in the current pregnancy. The HC group consisted of women who terminated their pregnancy for non-medical reasons, with a history of at least one prior successful pregnancy and no history of adverse pregnancy outcomes ($n = 27$), ensuring their suitability as healthy controls. Exclusion criteria for all participants included: age over 40 years, chromosomal abnormalities in either parent or embryo, anatomical abnormalities of the reproductive tract, history of autoimmune diseases, and recent infections or use of hormones/immunosuppressive drugs within the past three months. The clinical characteristics of both groups are summarized in Supplementary Table 2. PBMCs were isolated from peripheral blood using density gradient centrifugation with Ficoll-Hypaque (MP Biomedicals, Santa Ana, CA, USA) and analyzed via flow cytometry.

Decidua was processed to isolate decidual immune cells through mechanical grinding, with the remaining tissue prepared as paraffin sections for immunofluorescence staining.

Additionally, serum samples were collected from 64 women under 40 years old with no history of adverse pregnancy outcomes, who underwent their first IVF-ET at the Reproductive Hospital Affiliated with Shandong University. These samples were taken 12-16 days post-embryo transfer, confirmed by a positive β-HCG test. At this early stage of pregnancy (approximately 5 weeks), no pregnancy loss had yet occurred. Participants were classified based on pregnancy outcomes into two groups: 32 with normal pregnancies (HC group) and 32 with EPL (EPL group). The serum samples were specifically used to investigate the expression profiles of immune-related cytokines and cytotoxic molecules in early pregnancy.

Cell line culture

The HTR-8/SVneo immortalized human extravillous trophoblast cell line (ATCC CRL-3271, Manassas, VA, USA) was cultured in Dulbecco's modified Eagle medium-F12 Ham (DMEM/F12; Gibco, USA) supplemented with 10% heat-inactivated fetal bovine serum (FBS; Gibco, Grand Island, NY, USA) and 1% penicillin/streptomycin (HyClone, Logan City, UT, USA) in a 37 °C humidified incubator with 5% CO_2. In the present study, HTR-8/SVneo cells were used between passages 3 and 20.

Animal study

This study utilized an immunologically mediated spontaneous abortion mouse model[35,63], involving CBA/J female mice (Hua Fukang Biological Technology, Stock #11004 A), DBA/2 J male mice (Vital River Laboratory Animal Technology, Stock #214), and BALB/c male mice (Vital River Laboratory Animal Technology, Stock #211) aged 8-10 weeks. Mice were housed in a specific pathogen-free (SPF) barrier facility under controlled conditions (20–25 °C, 50% humidity, 12 h light/dark cycle), with no more than 6 mice per cage. Experimental and control groups were co-housed to avoid litter effects. During estrus, CBA/J female mice were mated with DBA/2 J male mice or BALB/c male mice, with the presence of a vaginal plug marked as embryonic day 0.5 (E0.5). Three experimental groups were defined in this study: 1) CBA/J female mice were mated with BALB/c male mice to establish a NP model ($n = 10$); 2) CBA/J female mice were mated with BALB/c male mice and injected intravenously with 5 mg/kg anti-mouse 4-1BB (BE0239; Bio X Cell) at E7.5 to establish a group of upregulated and functionally activated CD11c + CD8 + T cells ($n = 10$), which were used to investigate the relationship between changes in CD11c + CD8 + T cell numbers and the abortion phenotype[34,64]; and 3) CBA/J female mice were mated with DBA/2 J male mice to establish a classical AP model ($n = 10$). Pregnant mice were euthanized using carbon dioxide inhalation at E12.5, and the number of live fetuses and degree of embryo resorption were determined to calculate the rate of embryo resorption. Eye socket blood, decidua, and spleen samples were collected from pregnant mice. PBMCs were isolated from the mice via density gradient centrifugation and used directly for flow cytometry assays. For the decidua and spleen, the tissues were separately collected and processed using mechanical grinding to isolate decidual and splenic immune cells for flow cytometry experiments. Moreover, some embryonic tissues were collected at E12.5 for paraffin embedding and subsequent immunofluorescence staining. All of the animal experiments conformed to the requirements of the ethics committees of the Center for Reproductive Medicine of Shandong University (Ethical Review No. 116, 2022).

Flow cytometry

For phenotypic staining, human lymphocytes were stained with the following antibodies (all from BioLegend, used at 1:100 dilution unless otherwise stated): APC-conjugated anti-human CD3, APC/Fire™ 750-conjugated anti-human CD8, FITC-conjugated anti-human CD11c, PE-conjugated anti-human CCR7, BV421-conjugated anti-human CD45RA, PE-Cy7-conjugated anti-human CD38, Percp-conjugated anti-human HLA-DR, and BV875-conjugated anti-human PD-1. Mouse lymphocytes were stained with APC-Cy7-conjugated anti-mouse CD3, FITC-conjugated anti-mouse CD8, Percp-conjugated anti-mouse CD8, BV605-conjugated anti-mouse CD11c, BV421-conjugated anti-mouse CD103, PE-conjugated anti-mouse PD-1 and Percp-conjugated anti-mouse CD69 antibodies (all from BioLegend, used at 1:100 dilution unless otherwise stated).

For intracellular cytokine staining, human lymphocytes were stimulated with anti-human CD3 and anti-human CD28 antibodies (BioLegend, 1 μg/ml) for 8 hours at 37 °C in the presence of 5% CO_2. Brefeldin A (BioLegend, 5 μg/ml) and BV605-conjugated anti-human CD107a were added in the last 6 hours. The cells were permeabilized using a Cytofix/Cytoperm Kit (BD Biosciences) and stained with PE-conjugated anti-human Granzyme B, BV711-conjugated anti-human Perforin, PE-Cy7-conjugated anti-human TNF-α, and BV785-conjugated anti-human IFN-γ antibodies (all from BioLegend, used at 1:100 dilution unless otherwise stated). Similarly, mouse lymphocytes were stimulated with Cell Activation Cocktail (BioLegend, used as per manufacturer's instructions, containing optimized concentration of PMA, ionomycin, and brefeldin A) and PE-Cy7-conjugated anti-mouse CD107a for 6 hours in the presence of 5% CO_2. The cells were permeabilized using a Cytofix/Cytoperm Kit (BD Biosciences) and stained with BV421-conjugated anti-mouse Granzyme B, PE-conjugated anti-mouse Perforin, and APC-conjugated anti-mouse IFN-γ antibodies (all from BioLegend, used at 1:100 dilution unless otherwise stated). The data were obtained using a FACS-Fortessa (BD Biosciences) and analyzed via FlowJo version X (FlowJo, Ashland, OR, USA). Detailed information on all the antibodies used is provided in Supplementary Data 1.

Cell sorting and co-culture

PBMCs were isolated from healthy women ($n = 5$) with healthy early pregnancies, and APC-conjugated anti-human CD3 (BioLegend, 1:100 dilution), APC/Fire™ 750-conjugated anti-human CD8 (BioLegend, 1:100 dilution) and PE-conjugated anti-human CD11c (BioLegend, 1:100 dilution) antibodies were added to obtain CD11c + CD8 + T cells and CD11c-CD8 + T cells. Additionally, for decidual tissue samples from both healthy early pregnancy ($n = 3$) and EPL ($n = 3$) participants, single-cell suspensions were prepared. CD8 + T cells were labeled with APC-conjugated anti-human CD3 (BioLegend, 1:100 dilution) and APC/Fire™ 750-conjugated anti-human CD8 (BioLegend, 1:100 dilution) antibodies. After the cells were washed and filtered, they were transferred to sterile flow cytometry tubes and sorted using a FACSAria II flow cytometer (BD Biosciences).

Purified CD11c + CD8 + T cells and CD11c-CD8 + T cells from the peripheral blood of healthy early pregnant women, as well as purified CD8 + T cells from the decidual tissue of both healthy early pregnant and EPL participants, were seeded in 6-well plates containing RPMI 1640 medium (HyClone, Logan City, UT, USA) supplemented with 10% FBS (Gibco, Grand Island, NY, USA) and 1% penicillin/streptomycin (HyClone, Logan City, UT, USA). The cells were co-cultured with HTR-8/Svneo immortalized human trophoblast cells at a ratio of 1:1 using cell culture inserts (LabSelect, Beijing, China) of 0.4 μm pore size in 6-well plates. After incubation at 37 °C with 5% CO_2 for 36 hours, the suspended CD8 + T cells in the culture medium were collected for flow cytometry analysis.

Placental organoid culture

In this study, placental villous tissues were collected from healthy pregnant women at 6-8 weeks of gestation who opted for non-medical termination of pregnancy. The collected villous tissues were immediately placed in pre-cooled sterile saline and gently washed to remove blood clots and extraneous tissues, such as fetal membranes, while

preserving the integrity of the villous structure as much as possible. The villous tissues were then sequentially digested at 37 °C in a water bath using 0.25% trypsin (Gibco, USA) and 1 mg/mL collagenase V (Sigma-Aldrich, St. Louis, MO, USA) for 5 minutes each, with gentle pipetting to facilitate tissue dissociation. Enzymatic digestion was terminated by adding Advanced DMEM/F12 medium (Gibco, USA) supplemented with 10% fetal bovine serum (FBS). The cell suspension was then passed through a 100 μm filter to remove undigested tissue fragments. The filtrate was centrifuged at 400 × g for 5 minutes, the supernatant was discarded, and the cell pellet was resuspended in growth factor-reduced Matrigel (Corning, NY, USA) to establish a three-dimensional scaffold. Subsequently, 25 μL of the cell-Matrigel mixture was plated at the center of each well in a 24-well culture plate. The plate was incubated at 37 °C with 5% CO_2 for 20 minutes to allow Matrigel polymerization. Following polymerization, 500 μL of pre-warmed placental organoid culture medium[65,66] (composition detailed in Supplementary Table 3) was added to each well. The culture medium was refreshed every two days, and organoid growth was monitored regularly. Typically, placental organoids with characteristic cystic structures formed within 5-7 days. Organoid identity was validated by immunofluorescence staining with CK7 (1:200 dilution, ProteinTech, Wuhan, China), and F-actin was visualized using TRITC-conjugated phalloidin (100 nM, Yeasen, Shanghai, China). To investigate the effect of decidual CD8 + T cells on placental organoid formation, on day 2 (D2) of culture, CD8 + T cells isolated from the decidua of HC and EPL patients were introduced into the culture system using a non-direct contact co-culture approach for 36 hours. Organoid growth and morphological changes were observed and recorded under a microscope on days 4 (D4) and 6 (D6) of culture.

Matrigel-coated transwell invasion assays

The matrigel matrix (Corning, NY, USA) without growth factors was diluted 1:9 with DMEM/F12 medium (Gibco, USA) and pre-coated onto Transwell inserts (Corning, NY, USA) with an 8 μm pore size in 24-well plates. The inserts were then incubated at 37 °C for 1 hour. In the upper chamber, 250 μL of culture medium containing 0.1% FBS was used to seed 5×10^4 trophoblasts. A total of 750 μL of culture medium containing 10% FBS was added to the lower chamber, along with CD11C + CD8 + T cells, CD11C-CD8 + T cells, or CD8 + T cells isolated from peripheral blood and decidua, or treated with IFN-γ (10 ng/ml, Sigma–Aldrich, St. Louis, MO, USA) or pretreated with MCC950 (10 μM, Sigma–Aldrich, St. Louis, MO, USA) for 1 hour before IFN-γ treatment. Note that MCC950 is a selective inhibitor of pyroptosis[29]. After the cells were incubated at 37 °C with 5% CO_2 for 36 h, non-invading cells on the upper side of the membrane were gently removed with a cotton swab. The remaining cells were fixed with 4% paraformaldehyde (Solarbio, Beijing, China) for 30 minutes, air-dried, and then stained with 0.1% crystal violet (Solarbio, Beijing, China) for 15 minutes. The number of cells invading through the membrane was observed and imaged with an Olympus IX73 inverted microscope (Olympus Corporation, Tokyo, Japan). Five different fields were randomly selected in each insert for cell counting, and the average number of cells invading through the membrane was used to quantify the invasive ability of the cells in each experimental group.

Wound-healing assay

Co-cultured or IFN-γ (10 ng/ml, Sigma–Aldrich, St. Louis, MO, USA) -treated trophoblasts were seeded in 6-well plates until they reached an appropriate density. Using a 200 μL sterile pipette tip, a scratch was made in each well to create a cell-free wound area. The cells were gently washed twice with warm PBS to remove debris. Culture medium was added, and images were taken at specific time points using an Olympus IX73 inverted microscope (Olympus Corporation, Tokyo, Japan). The wound healing area was analyzed using ImageJ software (ImageJ Software Inc., MD, USA).

Human chorionic villous explant and primary EVT culture

Fresh chorionic villous tissue was collected from healthy pregnant women at 6-8 weeks of gestation who opted for artificial abortion due to their voluntary willingness. Before artificial abortion, fetal heartbeats were confirmed via abdominal ultrasound. The collected chorionic villi were washed with cold normal saline to remove blood clots and cut into approximately 2 mm fragments using ophthalmic scissors. The tissue fragments were then resuspended in DMEM/F12 medium (Gibco, USA) containing 1% penicillin/streptomycin (HyClone, Logan City, UT, USA) and 10% FBS (Gibco, Grand Island, NY, USA). The fragments were evenly plated in a 24-well plate pre-coated with 100 μL of Matrigel (Corning, NY, USA) diluted 1:1 with DMEM/F12 medium. Successful anchoring of the chorionic villous explants on Matrigel and the emergence of EVT cells from the tissue fragments defined the zero-hour sample. The explants were treated with or without IFN-γ (10 ng/ml, Sigma–Aldrich, St. Louis, MO, USA) or pretreated with MCC950 (10 μM, Sigma–Aldrich, St. Louis, MO, USA) for 1 hour followed by IFN-γ treatment. The outgrowth area of the explants was captured at 24 hours and 48 hours using an Olympus IX73 inverted microscope (Olympus Corporation, Tokyo, Japan) to evaluate EVT migration. The outgrowth area was quantified using ImageJ software (ImageJ Software Inc., MD, USA).

The remaining villous tissue was fragmented into 2 mm pieces and seeded into 60 mm culture dishes pre-coated with Matrigel diluted 1:9 with DMEM/F12 medium (Gibco, USA). The cells were cultured in DMEM/F12 medium containing 10% FBS (Gibco, Grand Island, NY, USA) and 1% penicillin/streptomycin (HyClone, Logan City, UT, USA) for 2-3 days. Once the villous fragments adhered to the dish and EVT cells were observed growing out from the villous fragments, the medium was changed every other day. When EVT cells reached a sufficient number, they were detached via 0.25% trypsin (HyClone, Logan City, UT, USA) to isolate human primary EVT cells. The purity of the isolated EVT cells was confirmed via immunofluorescence staining with the trophoblast and EVT-specific markers CK7 (1:200 dilution, ProteinTech, Wuhan, China) and HLA-G (1:200 dilution, Exbio, Prague, Czech Republic). In the present study, EVT cells between passages 2 and 8were used for follow-up experiments.

Quantitative polymerase chain reaction (qPCR)

Total RNA was extracted from samples using the RNA-Quick purification kit (YiShan Biotech, Shanghai, China). The concentration and purity of RNA were measured using a NanoDrop One spectrophotometer. Subsequently, 1 μg of RNA was reverse transcribed into 20 μL of complementary DNA (cDNA) using the PrimeScript RT reagent kit (Takara, Shiga, Japan) according to the manufacturer's instructions. qPCR was performed on a Roche LightCycler 480 System (Roche, Penzberg, Germany) in a total reaction volume of 10 μL, containing 1 μL of cDNA, 0.8 μL of specific primers, 5 μL of SYBR Green Master Mix (TaKaRa Bio), and 3.2 μL of RNase-free dH_2O. The cycling conditions were set as follows: initial denaturation at 95 °C for 10 minutes, followed by 40 cycles of denaturation at 95 °C for 10 seconds, annealing and extension at 60 °C for 1 minute. The melting curve analysis included one cycle of 95 °C for 10 seconds, 60 °C for 1 minute, and a final step of 95 °C for 15 seconds. The sequences of primers used are listed in Supplementary data 2.

Western blotting

Total protein was extracted from the samples using lysis buffer containing protease and phosphatase inhibitors (Cell Signaling Technology, MA, USA). The protein concentration was determined using a BCA protein assay kit (Thermo Fisher Scientific, MA, USA). Equal amounts of protein (10 μg) were separated by SDS-polyacrylamide gel electrophoresis and transferred to a 0.45 μm polyvinylidene difluoride (PVDF) membrane (Millipore, MA, USA). The membrane was blocked with 5% skim milk at room temperature for 1 hour to prevent nonspecific

binding. Subsequently, the membrane was incubated overnight at 4 °C with specific primary antibodies against the following proteins: α-Tubulin (1:1000 dilution, Santa Cruz Biotechnology, USA), NLRP3 (1:1000 dilution, Abcam, Cambridge, UK), c-Caspase-1 (1:1000 dilution, Abcam, Cambridge, UK), or GSDMD-N (1:1000 dilution, Abcam, Cambridge, UK). The next day, the membrane was incubated with HRP-conjugated secondary antibodies at room temperature for 1 hour. Protein signals were detected using Prolighting HRP reagents (Thermo Fisher, USA), and the signals were captured with a chemiluminescence imaging system (e-BLOT, Shanghai, China). The relative density of protein bands was analyzed using ImageJ software (ImageJ Software Inc., MD, USA).

Propidium iodide (PI) staining

Cells were cultured in 96-well plates until they reached an appropriate density. They were then divided into three groups: untreated, treated with IFN-γ (10 ng/ml, Sigma–Aldrich, St. Louis, MO, USA), and pre-treated with MCC950 (10 μM, Sigma–Aldrich, St. Louis, MO, USA) for 1 hour followed by IFN-γ treatment for 36 hours. After treatment, the cells were incubated with 5 μg/mL PI dye (Servicebio, China) at room temperature for 15 minutes in the dark. Following incubation, the cells were then incubated with 4′,6-diamidino-2-phenylindole (DAPI; Abcam, Cambridge, UK) for 5 minutes. After staining, the cells were observed under a fluorescence microscope (Olympus Corporation, Tokyo, Japan), and the proportion of PI-positive cells was calculated to assess cell death rates under different treatment conditions.

Scanning electron microscopy (SEM)

Trophoblasts subjected to different treatments were fixed with 2.5% glutaraldehyde solution (Servicebio, China) for 2 hours. The cells were then fixed with 1% osmium tetroxide (Ted Pella Inc., Redding, CA, USA) at room temperature for 1 hour. Following fixation, the cells underwent a graded ethanol dehydration series (30%, 50%, 70%, 90%, 100%, 100%), with each step lasting 15 minutes, followed by a 15-minute treatment with isoamyl acetate (Sinopharm Chemical Reagent Co. Ltd., Shanghai, China). After dehydration, the samples were subjected to critical point drying (K850, Quorum, UK) and then mounted onto conductive carbon adhesive tape. The samples were sputter-coated with gold for 30 seconds using an ion sputter coater (MC1000, HITACHI, Japan). The ultrastructural features of the cell surface were observed using a scanning electron microscope (SU8100, HITACHI, Japan), focusing on apoptosis-related morphological changes, such as cell membrane rupture and bubble formation, to assess trophoblast pyroptosis.

Haematoxylin–eosin (HE) staining

The paraffin-embedded mouse uterine tissue sections were deparaffinized by placing them in xylene twice for 5 minutes each. The sections were then rehydrated through a series of graded ethanol solutions (100%, 95%, 80%, and 70%) for 2 minutes each, followed by a 5-minute rinse in distilled water. Hematoxylin staining was conducted for 90 seconds, followed by a 5-minute rinse under running water to remove excess dye. The sections were briefly differentiated in 1% acid alcohol and then blued in tap water for 1 minute. The sections were subsequently stained with eosin for 15 seconds and quickly rinsed under running water to remove excess dye. The stained sections were dehydrated in 95% ethanol and absolute ethanol for 1 minute each and then cleared with two changes of xylene for 5 minutes each. Images were captured using the APERIO VERSA8 microscope (Leica, Wetzlar, Germany).

Immunofluorescence

Human decidual and mouse uterine tissues were fixed in 4% paraformaldehyde, dehydrated, embedded in paraffin, and sectioned into 5-6 μm paraffin sections. After baking, deparaffinization, and hydration, heat-mediated antigen retrieval with Tris/EDTA buffer (pH 9.0) was performed, followed by overnight incubation at 4 °C with specific primary antibodies against mouse-anti-human CD11c (1:200 dilution, ZSGB-Bio, Beijing, China), rabbit-anti-human CD8 (1:200 dilution, ZSGB-Bio, Beijing, China), or rabbit-anti-mouse CK7 (1:100 dilution, ProteinTech, Wuhan, China) separately. The sections were then incubated with fluorescently labeled secondary antibodies, including Alexa Fluor 488 and Alexa Fluor 594 (1:800 dilution, Thermo Fisher Scientific, USA), for 1 hour at room temperature. Nuclear staining was performed using DAPI (Abcam, Cambridge, UK), and images of immunofluorescence were obtained with the APERIO VERSA8 microscope (Leica, Wetzlar, Germany).

Detection of immune-related cytokines and cytotoxic molecules

The serum samples were analyzed using the LEGENDplex™ Human CD8/NK Panel multiplex bead array (BioLegend, San Diego, CA, USA). After thawing the serum samples at room temperature, they were processed according to the manufacturer's instructions. Briefly, 25 μL of each serum sample was mixed with pre-mixed beads coated with antibodies specific to target molecules, including IL-2, IL-4, IL-6, IL-10, IL-17A, IFN-γ, Fas, FasL, granzyme A, granzyme B, perforin, and granulysin. The samples were then incubated with biotinylated detection antibodies, followed by the addition of PE-labeled streptavidin to detect analytes bound to the beads. Finally, the samples were analyzed using flow cytometry. The concentration of each analyte was determined by comparing the median fluorescence intensity (MFI) of the beads to a standard curve with known concentrations. The results were analyzed using the BioLegend LEGENDplex™ Data Analysis Software Suite.

Bioinformatics analysis

In our study, the scRNA-seq dataset (GSE164449)[22] of decidual CD45+ cells from 3 healthy pregnancies and 3 EPL patients was reanalyzed using the Seurat R package (4.4.0). The cells were filtered on the basis of the following criteria: >300 genes and a percentage of mitochondrial genes <20% in the droplet data. To eliminate batch effects due to background contamination, a set of genes that tend to be expressed in ambient RNA (*PAEP*, *HBG1*, *HBA1*, *HBA2*, *HBM*, *AHSP*, and *HBG2*) was also removed. After filtering, the gene-barcode matrices of all the samples were integrated to eliminate batch effects between different donors. Specifically, data normalization was performed using Seurat's 'NormalizeData()', and 3000 shared highly variable genes were identified using the 'FindVariableFeatures()' function. The data were then scaled using the 'ScaleData()' function, and PCA dimensionality reduction was performed using the 'RunPCA()' function, with data integration using the Harmony package. PCA visualization elbow plots were generated using the 'ElbowPlot()' function, and the top 21 principal components were selected for principal component analysis and uniform manifold approximation and projection (UMAP) dimensionality reduction. A nearest neighbor graph using 21 dimensions of PCA reduction was computed with 'FindNeighbors()', and clustering was performed at a resolution of 0.50 using the 'FindClusters()' function. Conserved markers for each cluster were identified using 'FindAllMarkers()', and machine annotation was conducted using the scHCLlite package and the SingleR package. The cells were re-annotated based on the basis of the markers identified in the original publication and the results of machine annotation. To observe the expression of CD11c in decidual CD8 + T cells in both groups, the 'FeaturePlot()' and 'VlnPlot()' functions in the Seurat package, as well as ggplot2, were used for visualization, and differential expression analysis was performed using the DEsingle package.

Additionally, SMART-seq2 transcriptome sequencing data (RNA-seq) of CD11c + CD8 + T and CD11c-CD8 + T cell subsets from the peripheral blood of 3 healthy donors were downloaded from the Gene Expression Omnibus (GSE183022)[18]. We analyzed the DEGs between

the two cell populations using the DESeq2 R package and the enhancedVolcano R package. Heatmaps were generated using the ComplexHeatmap R package, and potential functional pathways were analyzed through functional enrichment and annotation based on GO and KEGG analyses via the ClusterProfiler R package. In the differential expression analysis, genes with a fold change >2, $P < 0.05$, and FDR < 0.05 were considered significant. For the GO and KEGG analyses, terms with $P < 0.05$ were considered significant.

Statistical analysis

All data were processed using SPSS version 26.0 (IBM SPSS Statistics for Windows, Armonk, NY, USA), GraphPad Prism version 8.0. (GraphPad Software, San Diego, CA, USA) and Python 3.12.0 (New Castle, DE, USA). The Kolmogorov-Smirnov test combined with histograms, was used to test the normality of data distribution. For normally distributed continuous variables between two groups, an independent t test (for unpaired data) and paired t test (for paired data) were used for comparisons. For non-normally distributed data between two groups, the Mann-Whitney U test (for unpaired data) and Wilcoxon signed-rank test (for paired data) were used. Categorical variables were compared using the chi-square test or Fisher's exact test. For comparisons involving more than two groups, the one-way ANOVA was used. Specificity and sensitivity were assessed using ROC analysis. $P < 0.05$ was considered statistically significant in all analyses. All experiments were performed at least three times independently.

Reporting summary

Further information on research design is available in the Nature Portfolio Reporting Summary linked to this article.

Data availability

All methods and data supporting the findings of this study are available within the manuscript and its supplementary information. This study did not generate new sequencing data. The scRNA-seq and bulk RNA-seq datasets used in this study were obtained from publicly available databases and can be accessed from the Gene Expression Omnibus (https://www.ncbi.nlm.nih.gov/geo/) under the accession codes GSE164449 and GSE183022. Source data are provided with this paper.

Code availability

The code used in this study is available on GitHub at https://github.com/zzwang1030/scRNA_BP, and archived on Zenodo with the DOI: 10.5281/zenodo.15622163[67].

References

1. Dimitriadis, E., Menkhorst, E., Saito, S., Kutteh, W. H. & Brosens, J. J. Recurrent pregnancy loss. *Nat. Rev. Dis. Prim.* **6**, 98 (2020).
2. ACOG Practice Bulletin No. 200 summary: Early pregnancy loss. *Obstet. Gynecol.* **132**, 1311–1313 (2018).
3. RPL, E. G. G. O. et al. ESHRE guideline: recurrent pregnancy loss. *Hum. Reprod. Open* **2018**, hoy004 (2018).
4. Quenby, S. et al. Miscarriage matters: the epidemiological, physical, psychological, and economic costs of early pregnancy loss. *Lancet* **397**, 1658–1667 (2021).
5. Deshmukh, H. & Way, S. S. Immunological basis for recurrent fetal loss and pregnancy complications. *Annu Rev. Pathol.* **14**, 185–210 (2019).
6. Wang, X. Q. & Li, D. J. The mechanisms by which trophoblast-derived molecules induce maternal-fetal immune tolerance. *Cell Mol. Immunol.* **17**, 1204–1207 (2020).
7. Tilburgs, T. et al. Human decidual tissue contains differentiated CD8+ effector-memory T cells with unique properties. *J. Immunol.* **185**, 4470–4477 (2010).
8. Wang, S. et al. The appropriate frequency and function of decidual Tim-3(+)CTLA-4(+)CD8(+) T cells are important in maintaining normal pregnancy. *Cell Death Dis.* **10**, 407 (2019).
9. Clark, D. A., Chaouat, G., Mogil, R. & Wegmann, T. G. Prevention of spontaneous abortion in DBA/2-mated CBA/J mice by GM-CSF involves CD8+ T cell-dependent suppression of natural effector cell cytotoxicity against trophoblast target cells. *Cell Immunol.* **154**, 143–152 (1994).
10. Arck, P. C., Merali, F., Chaouat, G. & Clark, D. A. Inhibition of immunoprotective CD8+ T cells as a basis for stress-triggered substance P-mediated abortion in mice. *Cell Immunol.* **171**, 226–230 (1996).
11. Wu, Z. et al. Pro-inflammatory signature in decidua of recurrent pregnancy loss regardless of embryonic chromosomal abnormalities. *Front Immunol.* **12**, 772729 (2021).
12. Lissauer, D., Kilby, M. D. & Moss, P. Maternal effector T cells within decidua: The adaptive immune response to pregnancy?. *Placenta* **60**, 140–144 (2017).
13. Ghafourian, M., Abuhamidy, A. & Karami, N. Increase of peripheral blood TCD8+ cells in women with recurrent miscarriage. *J. Obstet. Gynaecol.* **34**, 36–39 (2014).
14. Morita, K. et al. Analysis of TCR repertoire and PD-1 expression in decidual and peripheral CD8(+) T cells reveals distinct immune mechanisms in miscarriage and preeclampsia. *Front Immunol.* **11**, 1082 (2020).
15. Tilburgs, T. & Strominger, J. L. CD8+ effector T cells at the fetal-maternal interface, balancing fetal tolerance and antiviral immunity. *Am. J. Reprod. Immunol.* **69**, 395–407 (2013).
16. van der Zwan, A. et al. Mixed signature of activation and dysfunction allows human decidual CD8(+) T cells to provide both tolerance and immunity. *Proc. Natl Acad. Sci. USA* **115**, 385–390 (2018).
17. Rostamzadeh, D. et al. Altered frequency of CD8(+) CD11c(+) T cells and expression of immunosuppressive molecules in lymphoid organs of mouse model of colorectal cancer. *J. Cell Physiol.* **234**, 11986–11998 (2019).
18. Guo, A. L. et al. HIV-1-Specific CD11c(+) CD8(+) T Cells Display Low PD-1 Expression and Strong Anti-HIV-1 Activity. *Front Immunol.* **12**, 757457 (2021).
19. Lin, Y., Roberts, T. J., Sriram, V., Cho, S. & Brutkiewicz, R. R. Myeloid marker expression on antiviral CD8+ T cells following an acute virus infection. *Eur. J. Immunol.* **33**, 2736–2743 (2003).
20. Qualai, J. et al. Expression of CD11c is associated with unconventional activated T cell subsets with high migratory potential. *PLoS One* **11**, e0154253 (2016).
21. Kao, J. K., Hsue, Y. T. & Lin, C. Y. Role of new population of peripheral CD11c(+)CD8(+) T cells and CD4(+)CD25(+) regulatory T cells during acute and remission stages in rheumatoid arthritis patients. *J. Microbiol Immunol. Infect.* **40**, 419–427 (2007).
22. Chen, P. et al. The immune atlas of human deciduas with unexplained recurrent pregnancy loss. *Front Immunol.* **12**, 689019 (2021).
23. Wei, C. Y., Li, M. Q., Zhu, X. Y. & Li, D. J. Immune status of decidual macrophages is dependent on the CCL2/CCR2/JAK2 pathway during early pregnancy. *Am. J. Reprod. Immunol.* **86**, e13480 (2021).
24. Spathakis, M. et al. Spontaneous abortion is associated with differentially expressed angiogenic chemokines in placenta and decidua. *Arch. Gynecol. Obstet.* **308**, 821–830 (2023).
25. Li, Y. et al. RNA sequencing of decidua reveals differentially expressed genes in recurrent pregnancy loss. *Reprod. Sci.* **28**, 2261–2269 (2021).
26. Comins-Boo, A. et al. Functional NK surrogate biomarkers for inflammatory recurrent pregnancy loss and recurrent implantation failure. *Am. J. Reprod. Immunol.* **86**, e13426 (2021).

27. Guo, C. et al. Single-cell profiling of the human decidual immune microenvironment in patients with recurrent pregnancy loss. *Cell Discov.* **7**, 1 (2021).
28. Abdelsamed, H. A. et al. Human memory CD8 T cell effector potential is epigenetically preserved during in vivo homeostasis. *J. Exp. Med* **214**, 1593–1606 (2017).
29. Yuan, Y. et al. Curcumin improves the function of umbilical vein endothelial cells by inhibiting H(2)O(2)-induced pyroptosis. *Mol. Med. Rep.* **25**, 214, (2022).
30. Chiba, Y. et al. Caspase-4 promotes metastasis and interferon-gamma-induced pyroptosis in lung adenocarcinoma. *Commun. Biol.* **7**, 699 (2024).
31. Wang, S. et al. CTLA-4 blockade induces tumor pyroptosis via CD8(+) T cells in head and neck squamous cell carcinoma. *Mol. Ther.* **31**, 2154–2168 (2023).
32. Giampietri, C. et al. Analysis of gene expression levels and their impact on survival in 31 cancer-types patients identifies novel prognostic markers and suggests unexplored immunotherapy treatment options in a wide range of malignancies. *J. Transl. Med* **20**, 467 (2022).
33. Clouthier, D. L. et al. An interim report on the investigator-initiated phase 2 study of pembrolizumab immunological response evaluation (INSPIRE). *J. Immunother. Cancer* **7**, 72 (2019).
34. Choi, B. K. et al. Mechanisms involved in synergistic anticancer immunity of anti-4-1BB and anti-CD4 therapy. *Cancer Res* **67**, 8891–8899 (2007).
35. Wang, X. H. et al. Low chorionic villous succinate accumulation associates with recurrent spontaneous abortion risk. *Nat. Commun.* **12**, 3428 (2021).
36. Chen, L. et al. Decreased level of Eomes+dCD8+ T cells with altered function might be associated with miscarriage. *Reproduction* **162**, 107–115 (2021).
37. Takeda, Y., Azuma, M., Matsumoto, M. & Seya, T. Tumoricidal efficacy coincides with CD11c up-regulation in antigen-specific CD8(+) T cells during vaccine immunotherapy. *J. Exp. Clin. Cancer Res* **35**, 143 (2016).
38. Gao, L. et al. Decreased granzyme-B expression in CD11c(+)CD8(+) T cells associated with disease progression in patients with HBV-related hepatocellular carcinoma. *Front Immunol.* **14**, 1107483 (2023).
39. Zhang, M. et al. Development and validation of a visualized prediction model for early miscarriage risk in patients undergoing IVF/ICSI procedures: a real-world multi-center study. *Front Endocrinol. (Lausanne)* **14**, 1280145 (2023).
40. Yuan, G. et al. Prediction model for missed abortion of patients treated with IVF-ET based on XGBoost: a retrospective study. *PeerJ* **11**, e14762 (2023).
41. Marino, J. L. et al. Perinatal outcomes by mode of assisted conception and sub-fertility in an Australian data linkage cohort. *PLoS One* **9**, e80398 (2014).
42. Li, T. et al. Distinct mRNA and long non-coding RNA expression profiles of decidual natural killer cells in patients with early missed abortion. *FASEB J.* **34**, 14264–14286 (2020).
43. Li, D. et al. Genome-wide identification of microRNAs in decidual natural killer cells from patients with unexplained recurrent spontaneous abortion. *Am. J. Reprod. Immunol.* **80**, e13052 (2018).
44. Yougbare, I. et al. Activated NK cells cause placental dysfunction and miscarriages in fetal alloimmune thrombocytopenia. *Nat. Commun.* **8**, 224 (2017).
45. Laskarin, G. et al. Phenotype of NK cells and cytotoxic/apoptotic mediators expression in ectopic pregnancy. *Am. J. Reprod. Immunol.* **64**, 347–358 (2010).
46. Vinnars, M. T. et al. Enhanced Th1 and inflammatory mRNA responses upregulate NK cell cytotoxicity and NKG2D ligand expression in human pre-eclamptic placenta and target it for NK cell attack. *Am. J. Reprod. Immunol.* **80**, e12969 (2018).
47. Cao, L., Tang, Y., Niu, X., Guo, Q. & Huang, L. Mifepristone regulates macrophage-mediated natural killer cells function in decidua. *Reprod. Biol.* **21**, 100541 (2021).
48. Hu, W. T. et al. Decidual stromal cell-derived IL-33 contributes to Th2 bias and inhibits decidual NK cell cytotoxicity through NF-kappaB signaling in human early pregnancy. *J. Reprod. Immunol.* **109**, 52–65 (2015).
49. Huang, X. et al. Tissue-resident CD8(+) T memory cells with unique properties are present in human decidua during early pregnancy. *Am. J. Reprod. Immunol.* **84**, e13254 (2020).
50. Idali, F. et al. Impact of regulatory T cell therapy on immune cell composition and fetal survival rate in abortion prone mice. *Reprod. Fertil. Dev.* **35**, 504–517 (2023).
51. Yang, X. et al. IFN-gamma facilitates corneal epithelial cell pyroptosis through the JAK2/STAT1 pathway in dry eye. *Invest Ophthalmol. Vis. Sci.* **64**, 34 (2023).
52. Karki, R. et al. Synergism of TNF-alpha and IFN-gamma triggers inflammatory cell death, tissue damage, and mortality in SARS-CoV-2 infection and cytokine shock syndromes. *Cell* **184**, 149–168.e117 (2021).
53. Liu, J. & Yang, W. Mechanism of histone deacetylase HDAC2 in FOXO3-mediated trophoblast pyroptosis in preeclampsia. *Funct. Integr. Genomics* **23**, 152 (2023).
54. Sun, Y. et al. PINK1-mediated mitophagy induction protects against preeclampsia by decreasing ROS and trophoblast pyroptosis. *Placenta* **143**, 1–11 (2023).
55. Chen, Y. et al. TMBIM4 deficiency facilitates NLRP3 inflammasome activation-induced pyroptosis of trophoblasts: A potential pathogenesis of preeclampsia. *Biol. (Basel)* **12**, 208 (2023).
56. Jiang, Y. et al. Maternal exposure to ZIF-8 derails placental function by inducing trophoblast pyroptosis through neutrophils activation in mice. *Food Chem. Toxicol.* **187**, 114604 (2024).
57. Kim, Y. H., Choi, B. K., Kim, K. H., Kang, S. W. & Kwon, B. S. Combination therapy with cisplatin and anti-4-1BB: synergistic anticancer effects and amelioration of cisplatin-induced nephrotoxicity. *Cancer Res* **68**, 7264–7269 (2008).
58. Kim, Y. H. et al. Mechanisms involved in synergistic anticancer effects of anti-4-1BB and cyclophosphamide therapy. *Mol. Cancer Ther.* **8**, 469–478 (2009).
59. Practice committee of the american society for reproductive medicine. Electronic address, A. a. o. & practice committee of the american society for reproductive, M. The role of immunotherapy in in vitro fertilization: a guideline. *Fertil. Steril.* **110**, 387–400 (2018).
60. Achilli, C., Duran-Retamal, M., Saab, W., Serhal, P. & Seshadri, S. The role of immunotherapy in in vitro fertilization and recurrent pregnancy loss: a systematic review and meta-analysis. *Fertil. Steril.* **110**, 1089–1100 (2018).
61. Male, V., Gardner, L. & Moffett, A. Isolation of cells from the feto-maternal interface. *Curr. Protoc. Immunol.* **Chapter 7**, Unit 7 40–41-11 (2012).
62. Huhn, O. et al. Distinctive phenotypes and functions of innate lymphoid cells in human decidua during early pregnancy. *Nat. Commun.* **11**, 381 (2020).
63. Zhou, W. J. et al. Fructose-1,6-bisphosphate prevents pregnancy loss by inducing decidual COX-2(+) macrophage differentiation. *Sci. Adv.* **8**, eabj2488 (2022).
64. Compte, M. et al. A tumor-targeted trimeric 4-1BB-agonistic antibody induces potent anti-tumor immunity without systemic toxicity. *Nat. Commun.* **9**, 4809 (2018).
65. Sheridan, M. A. et al. Establishment and differentiation of long-term trophoblast organoid cultures from the human placenta. *Nat. Protoc.* **15**, 3441–3463 (2020).

66. Hu, C. et al. Endometrial BMP2 Deficiency Impairs ITGB3-mediated trophoblast invasion in women with repeated implantation failure. *Endocrinol.* **165**, https://doi.org/10.1210/endocr/bqae002 (2024).
67. Guo, L. et al. Enrichment of decidual CD11c+CD8+ T cells with altered immune function in early pregnancy loss. *Nat. Commun.* **GitHub**, https://doi.org/10.5281/zenodo.15622163 (2025).

Acknowledgements

We thank all participants for donating the research samples. This work was supported by grants from the National Key Research and Development Program of China (2024YFC2706700, 2022YFC2702400), the Excellence Research Group Program of NSFC (32588201), the National Natural Science Foundation of China (82471719), the Natural Science Youth Foundation of Shandong Province (ZR2023QH198), the specific research fund of The Innovation Platform for Academicians of Hainan Province (YSPTZX202310), and the Taishan Scholars Program for Young Experts of Shandong Province (tsqn202408396).

Author contributions

Y.L., JH.Y. and Z-J.C. conceived and designed the project; L.G., AL.G. and SW. H. performed the experiments and analyzed the data; L.G., AL.G. and YQ.G. collected the clinical tissue and serum samples; L.G. wrote the manuscript; Z-J.C., Y.L., JH.Y. and C.K. critically revised the manuscript. All the authors were involved in interpreting the data and had final approval of the submitted and published versions.

Competing interests

The authors declare no competing interests.

Additional information

Supplementary information The online version contains supplementary material available at https://doi.org/10.1038/s41467-025-61992-8.

Correspondence and requests for materials should be addressed to Zi-Jiang Chen, Junhao Yan or Yan Li.

Peer review information *Nature Communications* thanks the anonymous reviewer(s) for their contribution to the peer review of this work. A peer review file is available.